BIOCHEMISTRY
including biophysical chemistry & molecular biology

Article

pubs.acs.org/biochemistry

Self-Assembly of Aqueous Bilirubin Ditaurate, a Natural Conjugated Bile Pigment, to Contraposing Enantiomeric Dimers and M(−) and P(+) Tetramers and Their Selective Hydrophilic Disaggregation by Monomers and Micelles of Bile Salts

Michael W. Neubrand[†] and Martin C. Carey*

Department of Medicine, Harvard Medical School, and Division of Gastroenterology, Brigham and Women's Hospital and Harvard Digestive Diseases Center, Boston, Massachusetts 02115, United States

Thomas M. Laue

Department of Biochemistry, University of New Hampshire, Durham, New Hampshire 03824, United States

ABSTRACT: The solution behavior of bilirubin ditaurate (BDT), the first naturally occurring conjugated bile pigment to be physically and chemically characterized, was assessed in aqueous solution and in monomeric and micellar solutions of common taurine-conjugated bile salts (BS). Analytical ultracentrifugation revealed that BDT self-associates in monomer−dimer equilibria between 1 and 500 μM, forming limiting tetramers at low millimolar concentrations. Self-association was enthalpically driven with ΔG values of ≈5 kcal/mol, suggesting strong hydrophobic interactions. Added NaCl and decreases in temperature shifted the oligomerization to lower BDT concentrations. On the basis of circular dichroism spectra and the limiting size of the self-aggregates, we infer that the tetramers are composed of 2P(+) and 2M(−) enantiomeric BDT pairs in "ridge-tile" conformations interacting in a "double-bookend" structure. With added monomeric BS, blue shifts in the UV−vis spectra and tight isosbestic points revealed that BDT/BS heterodimers form, followed by BDT "decorating" BS micelles mostly via hydrophilic interactions. Conformational enantiomerism, fluorescence intensities, and anisotropy, as well as resistance of the hybrid particles to disaggregation in 6 M urea, suggested that two or three hydrogen-bonding sites bound BDT monomers to the hydroxyl groups of BS, possibly via pyrrole−π-orbital−OH interactions. BDT stabilized these interactions by enveloping the BS in its "ridge-tile" pincers with variable strain that maximized van der Waals interactions. Possibly because the BDT molecule becomes highly strained with BS subtending a 7β-hydroxyl group, BDT became totally resistant to oxidation in air. This work predicts that, because of BS dissolution of the BDT self-aggregates, BS/bilirubin hybrid particles, which are stabilized hydrophilically, are likely to be the dominant mode of transport for all conjugated bilirubins in bile.

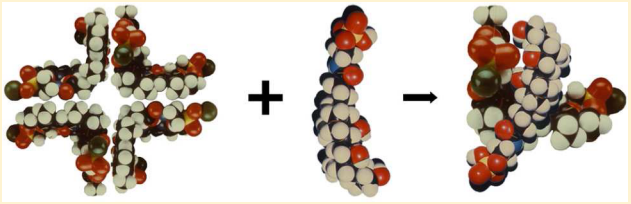

Bilirubin (Figure 1), which is the tetrapyrrolic end product of heme catabolism in higher organisms,[1] is excreted in bile following conjugation of one or both of its propionyl side chains with water-soluble acidic functional groups,[2,3] which are typically glucuronides (or glucoronosides) in mammals (Figure 1). The principal natural constitutional isomer is bilirubin IXα, so named because of the asymmetry of its methyl, vinyl, and propionyl side chains (Figure 1) corresponding to the parent protoporphyrin.[4] Conjugated bilirubins (cBR) account for more than 99% of bile pigments in bile.[5−7] Apparently, only small increases in the level of unconjugated bilirubin (UCB) in bile can exceed equilibrium solubility and initiate pigment gallstone formation.[8] It is believed[9] that hydrolysis of the glucuronyl ester linkage occurs either spontaneously at physiological pH[10] or, more likely, with endogenous or exogenous β-glucuronidase,[9] resulting in sparingly soluble UCB, which even in a slightly alkaline medium precipitates as insoluble calcium salts, usually $Ca(HUCB)_2$.[3,9] Secretion of cBR over a wide concentration range does not change the osmotic activity of rat[11] or monkey[12] bile, suggesting extensive self-association or a hybrid physicochemical state with BS micelles. In fact, on the basis of sucrose density gradient sedimentation, microfiltration, and gel-permeation chromatography, cBR in rat, human, and dog bile may be associated with BS micelles.[13−15] Nonetheless, the physicochemical states of pure cBR in aqueous systems have never been studied systematically,[16,17] principally because bulk synthesis and storage of BR glucuronosides have proven to be impossible.[18] For these reasons, we investigated the solution properties of a commercially available synthetic but natural bilirubin ditaurate (BDT) highly purified for this work. The molecule is a soluble, pH-insensitive, and relatively stable cBR (Figure 1). In BDT, bilirubin IXα is N-amide-linked with two molecules of the

Received: October 3, 2014
Published: January 28, 2015

DOI: 10.1021/bi501251v
Biochemistry 2015, 54, 1542−1557

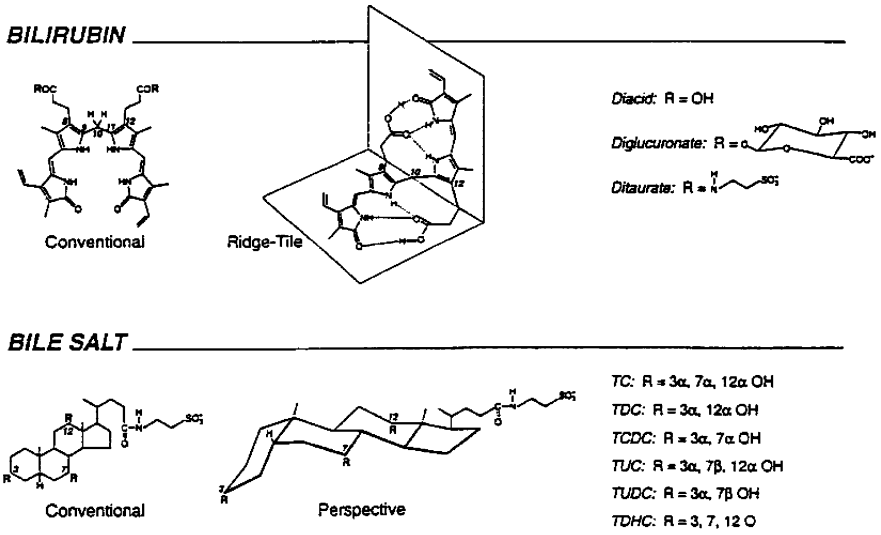

Figure 1. Conventional and three-dimensional drawings of bilirubin IXα and bile salt molecules. The bile salts that were studied were the *N*-amide taurine conjugates, which terminate in a single sulfonate charged group. TC, TDC, and TCDC have α-oriented OH groups at two (TCDC and TDC) or three (TC) positions (C3, C7, and/or C12). The urso prefixes (TUC and TUDC) indicate that the 7-OH function is β-oriented (equatorial). TDHC is a synthetic trioxo bile salt with no OH function. Bilirubin diglucuronate is the common diglucuronic acid conjugate of bilirubin IXα in human bile. It is shown for the purpose of comparison with bilirubin ditaurate, a natural conjugated bile pigment present in certain marine fish (e.g., *Seriola quinqueradiata*) that was studied systematically in this work.

amino acid taurine (2-aminoethanesulfonate). It was first synthesized by Jirsa and colleagues in Prague in 1956[19] and is used clinically as a chemical standard (from Porphyrin Products, renamed "Frontier Scientific", Logan, UT, in 1999) for bilirubin analysis. BDT is not present in human bile[5,6,8] but occurs naturally as the sole cBR in the bile of the yellowtail (genus *Seriola*) and related marine fish[20] and has been reported to be present in small quantities in chicken bile.[21]

Employing complementary physicochemical methods, we show that BDT molecules self-associate noncooperatively at micromolar concentrations to limiting tetramers at low millimolar concentrations. BDT monomers bind BS molecules tightly and "decorate" micellar BS as BDT monomers, thereby completely disassembling BDT dimers and tetramers. The binding is principally hydrophilic and resistant to 6 M urea, suggesting π-OH bonds formed by the π-electrons of BDT and the hydroxyl hydrogens of BS (Figure 1), or involving an intramolecular H-bonding lattice between the BS hydroxyls and H-bonds of BDT.[22−25] Interestingly, the susceptibility of BDT to oxidation in air was inhibited by BS species subtending 7β-OH functions, and as inferred by the circular dichroism (CD) spectra, BDT was forced into a more strained conformation when it was bound to these BS. This systematic study concerning two otherwise self-aggregating biliary lipids that, when mixed, form hybrid particles should provide a framework for further targeted experiments on the colloid−chemical properties of native mammalian biles.

EXPERIMENTAL PROCEDURES

Materials. Gram quantities of the disodium salt of BDT, specially purified by recrystallization for our experiments, were supplied in divided portions by Porphyrin Products. The chemical purity as well as that of UCB from the same source was 99% as determined by silica gel thin layer chromatography (TLC) (200 μg spots) (Analtech Corp., Newark, DE), developed in a $CHCl_3/CH_3OH/H_2O$ mixture [60:30:6 (v/v/v)]. UV−visible spectra of 10 mM solutions of UCB (pH ≈10.0) and BDT (pH ≈7.0) revealed no absorption bands in the 600−700 nm range, ruling out biliverdin contaminants. High-performance liquid chromatography (HPLC) employing 20 μL sample loop injections of 1 mM aqueous BDT and UCB (pH values given above), eluted with a 0.1 M dioctylamine/0.05 M glacial CH_3COOH mixture in a $MeOH/H_2O$ mixture [90:10 (v/v)], and absorbances (A) measured at 450 nm[26] revealed three constitutional isomers, IX-α, III-α, and XIII-α, present in 94, 2, and 4% proportions in the case of UCB and 75, 15, and 10% proportions in the case of BDT, respectively, with presumptive assignments based on data of McDonagh and Assisi.[27] To obtain spectra of individual BDT isomers, the HPLC-separated dioctylamine salts of BDT were diluted with solvent to ≈31 μM and scanned by employing a Cary 118C recording UV−vis spectrophotometer.

BS were the sodium salts of hydroxyl-substituted 5β-cholanoyl taurates, namely, taurocholate (3α,7α,12α-OH, NaTC), taurochenodeoxycholate (3α,7α-OH, NaTCDC), taurodeoxycholate (3α,12α-OH, NaTDC), tauroursо(7-epi)-cholate (3α,7β,12α-OH, NaTUC), tauroursodeoxycholate (3α,7β-OH, TUDC), and taurodehydro(triketo)cholate (3α,7α,12α-trioxo, NaTDHC) (Figure 1). They were purchased from Calbiochem (San Diego, CA) and Sigma Chemical (St. Louis, MO) or received as generous gifts (G. Salen and A. Batta, East Orange, NJ, and H. Falk, Freiburg, Germany). All BS, including NaTC,[28] were 96−99% pure as determined by TLC and HPLC, with the minor impurities being other conjugated BS. Emission spectrophotometry of 50 mM solutions in H_2O (natural pH) revealed fluorescent impurities of an uncertain chemical nature in all the solutions. We removed these to leave <4% of their original concentrations employing the procedure of Hsu,[29] based on the earlier approach of Kratohvil and DelliColli.[30] In brief, saturated solutions of BS in a 90% (v/v) $EtOH/H_2O$ mixture were washed thrice with powdered activated charcoal (Norit 211, particle size of 45−80 μm, Eastman Kodak Co., Rochester, NY), refluxed at 95 °C for 10−20 min, followed by "flash"

DOI: 10.1021/bi501251v
Biochemistry 2015, 54, 1542−1557

evaporation of the EtOH/H_2O azeotrope at 70 °C, and then freeze-dried.[29]

Organic solvents and other chemicals were HPLC and/or American Chemical Society (ACS) reagent grade (Fisher Scientific, Medford, MA). NaCl was roasted in a muffle furnace at 600 °C to oxidize and remove organic impurities. Urea (Gallard Schlesinger, Carle Place, NY) and NaCl (Sigma Chemical) were free of chromophoric and fluorophoric impurities as determined by UV−vis and emission spectrophotometry, and argon (Yankee Oxygen, Cambridge, MA) was 99.99% pure. H_2O was filtered, deionized, and glass-distilled (Corning Glass, Corning, NY), and glassware was washed (24−48 h) in 2 M KOH dissolved in an EtOH/H_2O mixture [1:1 (v/v)] followed by 1 M HNO_3, rinsed in running distilled and deionized H_2O, oven-dried, and wrapped in aluminum foil.

Methods. The specially purified BDT was from a single ≈20 g lot (0211787) and received in sealed actinic ampules in ≈80 portions of ≈0.25 g each. Porphyrin Products (J. Bommer, personal communications, 1987 and 1989) certified that, after a proprietary cleanup step, BDT was purified by repeated precipitation from EtOH/H_2O mixtures. BDT was reported to be free of UCB (by HPLC) and believed to contain 3% bilirubin monotaurate but no free taurine (as determined by ninhydrin analysis); however, we found no bilirubin monotaurate or free taurine using TLC (see below). Within days of receipt, a number of ampules were opened, and ≈50−400 μM stock solutions were composed in H_2O at natural pH. We conducted dry weight determinations on the wet powder and on the aqueous solutions. The latter was prepared as weight per volume, followed by reduced-pressure drying at 110 °C, cooling, and reweighing as a function of time until the weight versus time curves reached a plateau. This approach assumed that anhydrous BDT was present after drying and that BDT was fully hydrated following equilibration with the laboratory environment. From multiple dry weight determinations employing quadruplicate 100 μL samples prepared gravimetrically, the differences between intended and analytic BDT weights were 3.5−3.9% with a mean of 3.8% (n = 5). This is close to the 3.6% moisture content found in BDT samples from the same source by thermogravimetric analysis.[31] Thereafter the formula M_r [apparent molecular weight (see eq 2)] was corrected for the moisture in each sealed BDT sample (approximated as 2 mol of H_2O/mol of BDT). The absorbance (A) values of identical BDT solutions from the same lot remained constant within 2% after experimentation for 2 years.

Aqueous stock solutions of BDT were prepared gravimetrically. Aqueous solutions (10 or 50 mM) of BS were composed in H_2O with and without NaCl and urea. Depending upon experimental conditions, these were diluted with a BDT stock solution to give a series of micellar or monomeric BS concentrations[30,32−35] at constant BDT, NaCl, and urea concentrations. The pH was adjusted to 7.6−8.0 with a few microliters of 1 M NaOH. Preparation of several UCB solutions over the pH range of 6.9−10.5 in micellar BS, and other experimental conditions for working with bile pigments, were similar to those described previously.[36] We boiled H_2O to remove O_2 and CO_2 and bubbled solutions with Ar during cooling. Stock solutions were blanketed and bubbled with Ar throughout each experiment. Analytic samples were prepared under subdued light and wrapped in aluminum foil, and experiments were performed in the dark. As inferred from the reproducibility of the spectrophotometric curves, BDT and UCB systems remained stable for at least 3 h under these conditions.

Absorption spectra were recorded employing a Cary 118C UV−visible spectrophotometer (Varian Associates, Palo Alto, CA) and a Hewlett-Packard (Palo Alto, CA) model 8452A diode-array spectrophotometer. BDT absorbances were kept between 0.05 and 2 units, and matched glass cuvettes with path lengths of 1−10 mm were employed. The slit width was adjusted by autocontrol. After pre-equilibration at the desired temperatures, the temperature of experimental cuvettes and blanks was controlled to ±0.05 °C by recirculating H_2O from a calibrated thermostated heat exchanger (D-2/RD, Lauda, Königshafen, Germany). For UV−vis scanning at temperatures other than room temperature (23 ± 1 °C), solutions were equilibrated for a further 4 min in prewarmed or precooled cuvettes. For conventional BDT spectra, a reference cuvette containing solvent was utilized, whereas equal concentrations of BDT in both sample and reference cuvettes were employed for difference spectra, with varying BS concentrations in the sample cuvette.

Fluorescence emission spectra were recorded on a PerkinElmer (Norwalk, CT) spectrofluorimeter (model MPF-66), employing an emission wavelength of 530 nm (slit width of 5 nm) and an excitation wavelength of 490 nm (slit width of 10 nm). Path lengths in the exciting and emitting beams were 3 and 10 mm, respectively. BDT concentrations were <40 μM, so that A_{490} and A_{530} did not exceed 0.2 and 0, respectively. Corrections for "inner-filter effects" used appropriate correction factors of Knudsen et al.:[37]

$$\mathrm{RFI}_{corr} = \mathrm{RFI}_{obs} \times 10^{A_1 d_1} \quad (1)$$

where subscripts denote the corrected and observed relative fluorescence intensities (RFI) and the superscript denotes the product of the respective absorbance at the excitation wavelength, A_1, times the half-path length of the excitation beam within the cuvette (d_1). Equation 1 gives correction factors that are accurate within 1% with A values of <0.2.[38]

Polarization measurements were performed with an 8000 C spectrofluorimeter (SLM Instruments, Urbana, IL) equipped with a Corning Glass cutoff filter (No. 3-69). We employed a 3 mm × 3 mm cuvette with excitation and emission slit widths of 4 and 16 nm, respectively. BDT polarization was measured by excitation at 490 nm, with emission monitored at 530 nm parallel and perpendicular to the plane of excitation. Anisotropy ratios were calculated according to the methods of Lakowicz.[39]

Circular dichroism (CD) spectra were recorded on a Cary 61 spectropolarimeter with sensitivities set at either 0.02 or 0.05 and automatic slit width control. The light path length was 5 mm, and BDT or UCB concentrations were 50 μM, the latter with micellar BS at pH 6.9−10.5 and A_{450} values of <1.2.

Sedimentation equilibrium experiments were conducted using a model E analytical ultracentrifuge (Spinco Division, Beckman Instruments, Palo Alto, CA) equipped with Rayleigh interference optics, a photoelectric scanner, Rotor Temperature Indicator and Control (RTIC), electronic speed control, and a He−Ne laser light source.[40] Interferograms were recorded employing Eastman Kodak Co. technical Pan film. High-speed experiments were performed essentially as described by Yphantis.[41] For each experiment, three solution/solvent pairs were examined using a six-channel, 12 mm thick, charcoal-filled Epon centerpiece with sapphire windows. The experimental temperature was 23.3 °C, and centrifugal speeds were 40000, 44000, 48000, and 52000 rpm. Because of its small M_r, BDT

DOI: 10.1021/bi501251v
Biochemistry 2015, 54, 1542−1557

could be dialyzed across the membrane of the double-sector ultracentrifugation cell. Therefore, solvent (buffer) and analytic solutions were designed to contain very dilute and more concentrated BDT solutions, respectively. Solutions were prepared quantitatively with corresponding volumes of buffer [1 or 100 mM NaCl with 20 mM Tris-HCl (pH 8.0)] by dilution of appropriate BDT stock solutions, with corrections for moisture as described above (see Methods). The ratios of the lowest neutral electrolyte concentration to BDT concentration were sufficient to minimize charge−charge nonideality and to act as a density stabilizer.[38] At the end of the experiments, UV−vis absorption scans at 660 nm ensured that no biliverdin ditaurate had formed.

Analysis of 200−300 fringe displacements from each interferogram was performed using an automated plate reader at a radial spacing, employing cell coordinates of 10 μm.[42] For studies at low micromolar BDT concentrations, a photoelectric scanner was employed. Approximately 40−50 absorbance measurements at 423 nm were collected between the cell's meniscus and the FC-43 fluorocarbon at the base of the channel.[43] The edited data (REEDIT program, kindly provided by D. Yphantis, Storrs, CT) were analyzed using NONLIN to provide values and 65% confidence intervals for the fitted parameters.[44] This program facilitated simultaneous fitting of data from one or more channels, all at different loading concentrations, radial positions, and angular velocities. The confidence intervals reflect the precision of the fit of a particular model to the experimental data and do not necessarily reflect the accuracy of each determination.

A model consisting of a single thermodynamically ideal component (i.e., BDT) was used.[44] This model provided the reduced apparent molecular weight (σ), defined as

$$\sigma = [M_r(1 - \bar{\nu}\rho)\omega^2]/(RT) \quad (2)$$

where M_r is the apparent molecular weight of BDT, $\bar{\nu}$ its partial specific volume (see below), ρ the solution density, and ω the angular velocity of the rotor.[45]

The ρ value of the solvent and $\bar{\nu}$ value of BDT molecules in solution were measured using a Mettler/Parr (Graz, Austria) precision density meter (model DMA O2D). Temperatures were maintained at 23.3 ± 0.01 °C using recirculated H_2O from two thermostated water baths connected in series. Density measurements were performed in triplicate at each of three or four BDT concentrations in either distilled H_2O or buffer [100 mM NaCl and 20 mM Tris-HCl (pH 8.0)]. Values of $\bar{\nu}$ were calculated according to the formula of Chervenka,[43] employing the slope of the graph plotting density as a function of BDT concentration.

$$\bar{\nu} = 1 - \text{slope}/\rho_{solv} \quad (3)$$

where ρ_{solv} corresponds to the density of the solvent. The $\bar{\nu}$ value for BDT (determined to three significant figures) was 0.677 in distilled H_2O (23.1 °C) and 0.661 in 100 mM NaCl and 20 mM Tris-HCl (pH 8.0).

RESULTS

UV−Vis Spectrophotometry of BDT. Figure 2A shows absorption spectra of BDT's constitutional isomers as purified ion pairs in 0.14 M dioctylamine [70:30 (v/v) MeOH/H_2O, pH 8.3 ± 0.3]. The figure assumes designations based on HPLC retention times of the corresponding UCB isomers.[27] The wavelengths of maximal absorption (λ_{max}) of the bilirubin

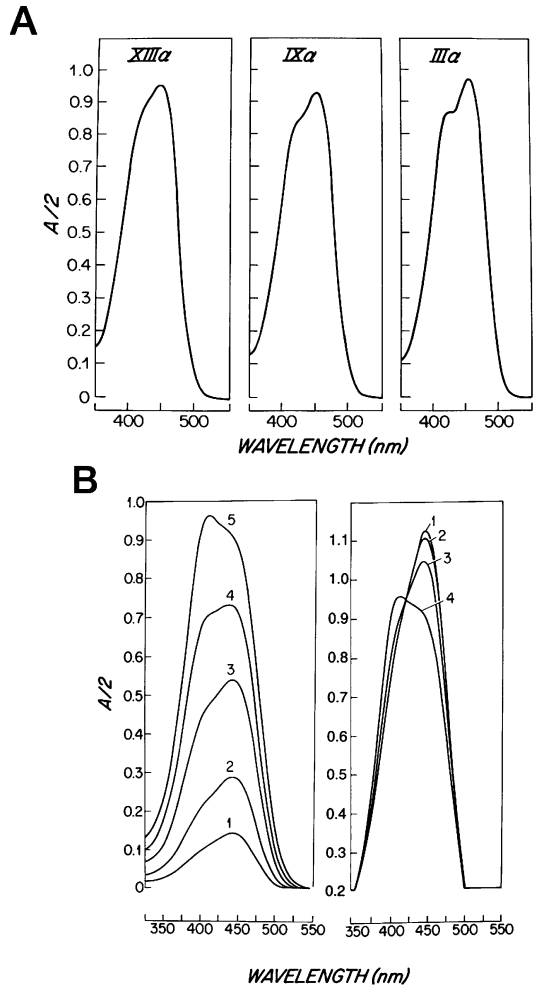

Figure 2. UV−visible absorption spectra of BDT. (A) Constitutional isomers of BDT, (a) IIIα, (b) IXα, and (c) XIIIα, in the disproportionated mixture as dioctylamine salts (23 ± 1 °C, pH 7.9−8.5). Each isomer was isolated as an ion pair following HPLC separation, dried, and redissolved in a 70:30 (v/v) CH_3OH/H_2O mixture to give a solution containing 0.14 M dioctylamine and each isomer at ≈31 μM. Derived assignments are based on HPLC retention times of UCB isomers. (B) UV−visible absorption spectra of BDT in H_2O (pH 7.6−8.0, 23 ± 1 °C). (left panel) The numbered spectra correspond to BDT concentrations of 50, 100, 200, 300, and 400 μM (1−5, respectively) with a constant (1 mm) light path length. (right panel) Cuvettes of different path lengths were used to give a constant value for the product of path length and BDT concentration. Numbered spectra correspond to BDT concentrations and path lengths of 40 μM and 10 mm, 80 μM and 5 mm, 200 μM and 2 mm, and 400 μM and 1 mm, respectively. A tight isosbestic point is present at 423 nm, indicating an equilibrium of only two physicochemical species in the system.

constitutional isomers differ, being 447 nm for IIIα, 450 nm for IXα, and 453 nm for XIIIα. A shoulder at 420 nm is present in all spectra, being most pronounced in BDT XIIIα, the exovinyl isomer, and least pronounced in BDT IIIα, the endovinyl isomer.

Figure 2B demonstrates the influence of BDT concentration on UV−vis spectra. The left panel displays absorbance spectra of 50−400 μM BDT in H_2O at 23 ± 1 °C with a constant (1 mm) light path length. With increasing BDT concentrations, λ_{max} shifts from 450 to 442 nm (curves 1 → 5), and the

DOI: 10.1021/bi501251v
Biochemistry 2015, 54, 1542−1557

shoulder at 415 nm becomes more pronounced, forming a blue-shifted λ_{max} at 413 nm in 400 μM BDT. The actual λ_{max} transition is not shown but occurred approximately midway between curves 4 and 5 (361 μM). The right panel of Figure 2B displays overlapped spectra of 40−400 μM BDT, where the product of the light path length and BDT concentration is held constant. It is to be noted that curves 1−4 intersect at a tight isosbestic point of 423 nm.

Figure 3A plots the dependencies of the apparent "aggregation numbers", that is, the numbers of monomers per BDT self-aggregate, for BDT concentrations of 12 μM to 3 mM (expressed as positive integers) in 1 mM NaCl [pH 8.0 (○)] and 100 mM NaCl and 20 mM Tris-HCl [pH 8.0 (●)]. Aggregation numbers were obtained by dividing the measured M_r by the calculated anhydrous M_r of the BDT monomer. At the lowest BDT and neutral electrolyte concentrations, the aggregation number approaches that of BDT monomers (M_r of BDT dianion of 797, M_r of BDT dianion with two Na^+ counterions of 843, and measured M_r value of 831). At the higher ionic strength (●) but for the same BDT concentration range, the aggregation numbers approximate those expected for a dimer or an equilibrium of monomers and dimers (Figure 3A, left sets of filled symbols). Aggregation numbers approach those for a tetramer at the highest BDT concentrations and at the higher ionic strength. These results imply that, at the most dilute (12−25 μM) BDT concentrations studied by UV−vis spectrophotometry, BDT is predominantly monomeric [Figure 3A (○)]. BDT concentrations probably correspond to the monomer−dimer equilibrium range in H_2O, where the blue shoulder became the λ_{max} in the UV−vis spectra (Figure 2B, left panel, curves 4 and 5). At the highest BDT concentrations [Figure 3A (●)], tetramers are present, most likely from dimerization of dimers (see Discussion); this BDT concentration range was outside the concentration limits of the UV−vis spectrophotometric experiments.

Figure 3B plots the dependence of BDT aggregation numbers on NaCl concentration (10−200 mM). Aggregation numbers of BDT [1.1 mM (○) and 1.6 mM (●) at pH 8.0] were determined interferometrically. At low NaCl concentrations, BDT is dimeric, and at high NaCl concentrations just below the salting-out limit, BDT is mainly tetrameric. Intermediate NaCl concentrations resulted in nonstoichiometric aggregation numbers, suggesting an equilibrium of BDT dimers and tetramers only.

Figure 3C shows the influence of temperature on BDT self-association. λ_{max} values from UV−vis spectra are plotted as a function of increasing BDT concentration (expressed as 8 + log[BDT] in molar) in H_2O and temperature (5−50 °C, top to bottom, respectively, on the left side of the curves). For low BDT concentrations, λ_{max} was constant, centered at 450 nm, but at higher BDT concentrations, λ_{max} shifted to the blue and a new λ_{max} dominated the spectra between 410 and 420 nm. As temperature was increased, the λ_{max} transition occurred at progressively higher BDT concentrations, ranging from 170 μM at 5 °C to an extrapolated value of 1 mM at 50 °C. Therefore, with stepwise increases in temperature, BDT self-association was progressively suppressed. Dimerization constants (K_D) were obtained utilizing the BDT concentrations at the inflection points, and from these, standard thermodynamic functions were calculated (Table 1). These data (Table 1) reveal that the negative free energy change (ΔG_D) upon dimerization resulted principally from a large negative enthalpy term (−4.80 to −4.43 kcal/mol), which decreases slightly with elevations in temperature.

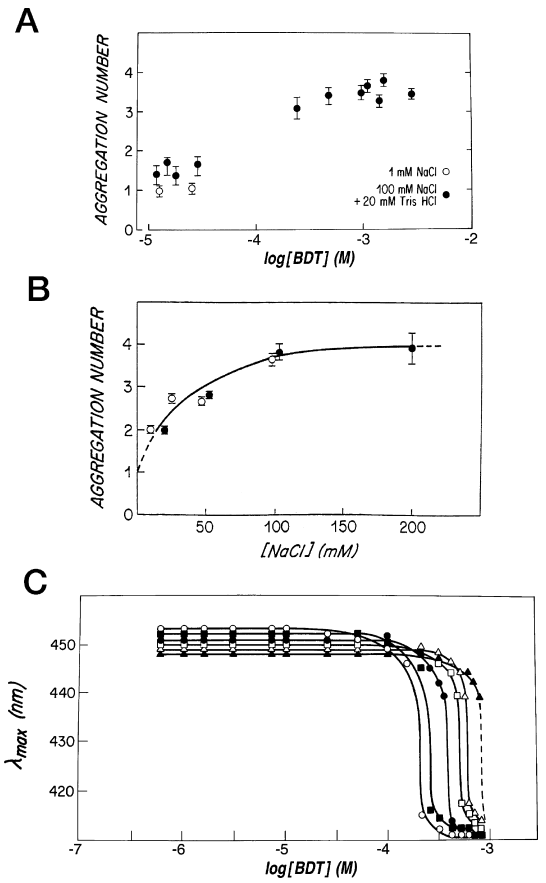

Figure 3. BDT aggregation numbers. (A) Mean numbers of BDT molecules per self-aggregate shown as a function of BDT concentration, expressed as positive integers at 23.3 °C and pH 8.0. BDT was dissolved in 1 mM NaCl (○) or 100 mM NaCl and 20 mM Tris-HCl (●). Examination was by means of a Beckman analytic ultracentrifuge at 23.3 °C with rotor speeds of 40000, 44000, 48000, and 52000 rpm using either a UV−visible scanner (8 + log[BDT] < 4) or Rayleigh interference optics (8 + log[BDT] > 4). Each aggregation number was obtained from the ratio of the apparent anhydrous molecular weight ($M_{r\ app}$) from eq 2 to the anhydrous monomer molecular weight ($M_{r\ mon}$). At low BDT concentrations in H_2O and 1 mM NaCl (○), BDT was predominantly monomeric in solution, whereas at all the highest concentrations in 100 mM NaCl and 20 mM Tris-HCl (●), the self-aggregate was predominantly a tetramer. (B) Influence of added NaCl on BDT aggregation numbers [10−200 mM NaCl and 20 mM Tris-HCl (pH 8.0)]. Self-aggregation of BDT was examined by analytic ultracentrifugation (conditions as described for panel A). Interferometrically derived BDT concentrations were 1.1 mM (○) and 1.6 mM (●). (C) Influence of BDT concentration and temperature on λ_{max} of BDT solutions in H_2O (pH 7.6−8.0). Temperatures were 5, 10, 20, 30, 40, and 50 °C (top to bottom, respectively, at the left side of the curves). With increases in temperature, λ_{max} shifts to the blue, and the BDT concentrations at the inflection points of the curves (equivalent to K_D) increase monotonically.

Influence of Added NaCl and Urea on BDT Self-Association. Figure 4 summarizes several sets of UV−vis spectra (A−D) under different solvent and BDT conditions (23 ± 1 °C, pH 7.6−8.0). Panel A shows that, with increasing BDT concentrations (0.6−50 μM) in 150 mM NaCl, a 415 nm blue-shifted λ_{max} becomes dominant between 25 and 50 μM [at 40 μM actually (not displayed)], which contrasts with an

DOI: 10.1021/bi501251v
Biochemistry 2015, 54, 1542−1557

Table 1. Thermodynamic Properties of BDT Self-Association[a]

T (°C)	ΔG_D[b]	ΔH_D[c]	$T\Delta S_D$[d]
5	−4.80	−5.87	−1.07
10	−4.75	−6.19	−1.44
15	−4.72	−6.02	−1.30
20	−4.70	−6.02	−1.35
25	−4.65	−6.04	−1.39
30	−4.64	−5.88	−1.24
35	−4.63	−6.28	−1.65
40	−4.65	−5.98	−1.33
50	−4.43	−6.36	−1.93

[a]Conditions: distilled H_2O, no buffer, pH ≈7.0. [b]ΔG_D corresponds to the change in free energy, calculated as $\Delta G_D = 2.303RT \log K_D$ (kilocalories per mole). [c]ΔH_D corresponds to the change in heat content (enthalpy) when 1 mol of BDT monomers aggregates to form a dimer. For these calculations, the K_D increment for a 10 °C increase in temperature was obtained from the tangent to the curve plotting K_D vs temperature. $\Delta H_D = [-RT^2\, \mathrm{dln}(K_D)]/(\mathrm{d}t)$. [d]$T\Delta S_D$ corresponds to the change in entropy associated with dimerization and follows the Gibbs relationship $T\Delta S_D = \Delta H_D - \Delta G_D$.

analogous transition at 361 μM in H_2O (Figure 2B). Figure 4B shows the UV−vis spectra of 100 μM BDT for which stepwise increases in NaCl concentration (from 0 to 600 mM, the latter approaching the salting-out limit) cause A_{450} to decrease markedly with reciprocal increases in A_{415}. This supports the concept that the BDT monomer−dimer equilibrium shifts toward the higher-order compounds, i.e., dimer−tetramer aggregates, with progressive increases in NaCl concentration. When enlarged (not shown), the overlapped spectra of Figure 4B are actually consistent with two "isosbestic points": one between curves 1 and 3 at ≈423 nm, the same wavelength as in pure H_2O (Figure 2B, right panel), and a second between curves 4 and 6 at ≈421 nm. Figure 4C displays the partial spectra of 100−400 μM BDT in 6 M urea, where a minor blue-shifted 415 nm shoulder is present in all spectra, identical to that of monomeric BDT in H_2O (Figure 2B, right panel). Progressive hyperchromia is the only concentration-dependent change in 6 M urea (Figure 4C), indicating inhibition of BDT self-aggregation (see Discussion). Figure 4D shows the UV−vis spectra of BDT in 6 M urea with added 150 mM NaCl, wherein the inorganic electrolyte concentration leads to a small increase in the magnitude of the 415 nm shoulder (compare with Figure 4C). Note that in panels C and D of Figure 4, BDT concentrations are identical for spectra 1 and 3, 2 and 4, 3 and 5, and 4 and 6.

Interactions of BS with BDT. Figure 5A (left panel) shows UV−vis spectra of 100 μM BDT with added monomeric concentrations (0−5 mM) of NaTC in H_2O. Increases in BS concentration decrease A_{max} and induce a shift in magnitude of the the blue shoulder of BDT to 420 nm, resulting in a tight isosbestic point at 427 nm. These spectral changes are specific and not BS-induced ionic strength effects because they differ from those induced by NaCl alone (Figure 4B). Experiments with monomeric solutions of other taurine-conjugated BS (NaTDC, 0−3.5 mM; NaTUDC, 0−5 mM; NaTCDC, 0−2 mM; and NaTDHC, 0−30 mM)[34] produced similar results, all showing identical isosbestic points at 427 nm (spectra not displayed). The right panel of Figure 5A (curves 2−7) displays BDT spectra with increasing concentrations of micellar NaTC (8−33 mM), where the critical micellar concentration (CMC) of NaTC in H_2O is ≈7.5 mM.[34,35] Of note is the fact that the blue-shifted shoulder in the BDT spectra with monomeric

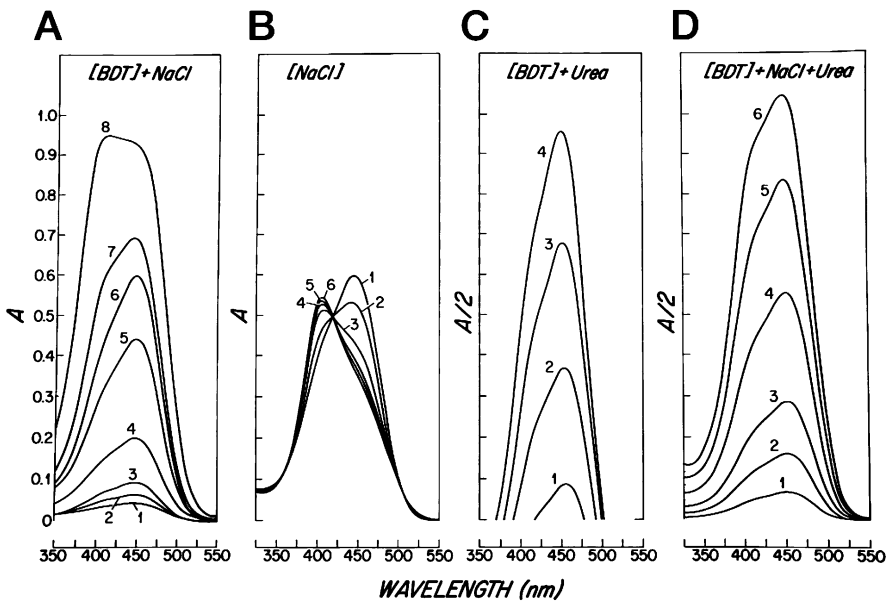

Figure 4. UV−visible absorption spectra of BDT for different solvent conditions (23 ± 1 °C, pH 7.6−8.0). (A) A series of BDT concentrations in 0.15 M NaCl, with numbered spectra corresponding to BDT concentrations of 0.6, 1, 1.6, 3, 7, 10, 25, and 50 μM (1−8, respectively; light path length of 10 mm; absorbance range of 1 for spectra 1−6 and 2 for spectra 7 and 8). (B) A single concentration of BDT (100 μM), with numbered spectra corresponding to increasing NaCl concentrations of 0, 10, 80, 150, 300, and 600 mM (1−6, respectively; light path length of 2 mm). Apparently, two isosbestic points are present, suggesting one intersection (curves 1−3) at 423 nm and the other (curves 4−6) at 431 nm. (C) A series of BDT concentrations in 6 M urea with numbered (partial) spectra corresponding to BDT concentrations of 100, 200, 300, and 400 μM (1−4, respectively; light path length of 1 mm). The absorbance range was 2, and zero suppression was 0.5. (D) Same experiment as in panel C but with added 150 mM NaCl (light path length of 1 mm). The numbered spectra correspond to BDT concentrations of 20, 50, 100, 200, 300, and 400 μM (1−6, respectively).

DOI: 10.1021/bi501251v
Biochemistry 2015, 54, 1542−1557

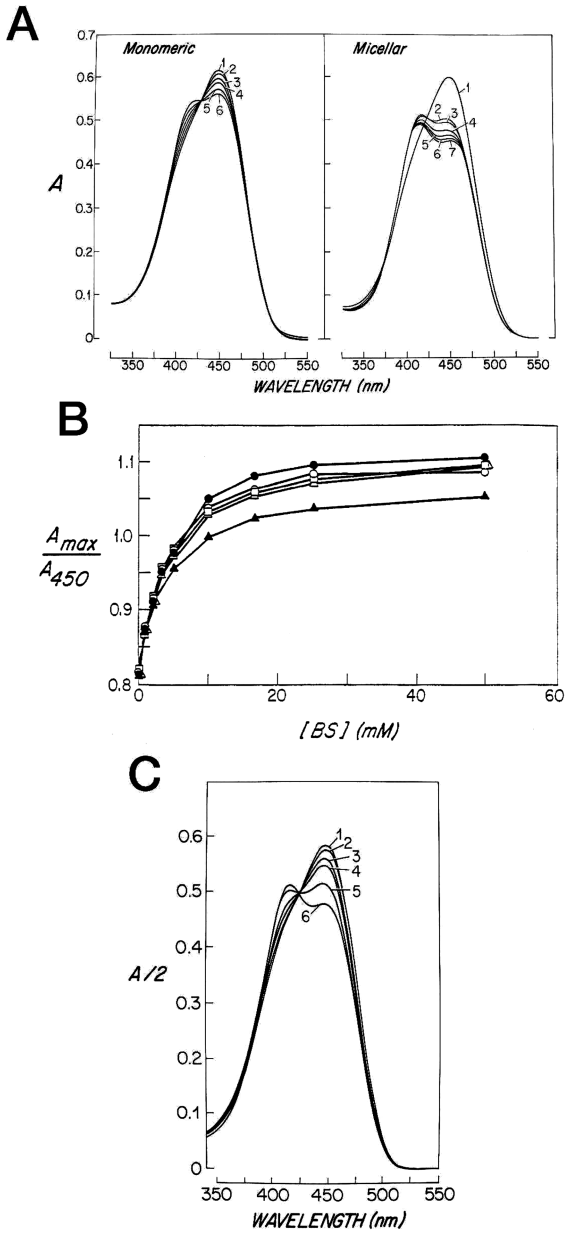

Figure 5. BDT–BS interactions. (A) UV–visible absorption spectra of 100 μM BDT in H_2O as a function of NaTC concentration (path length of 2 mm, 23 ± 1 °C, pH 7.6–8.0). In the left panel, numbered BDT spectra correspond to monomeric NaTC concentrations of 0, 0.5, 1, 2, 3.1, and 5 mM (1–6, respectively). An isosbestic point is present at 427 nm. The right panel shows spectra of BDT with increasing concentrations of micellar NaTC corresponding to NaTC concentrations of 0, 8, 11.1, 16.7, 25, 33.3, and 50 mM (1–7, respectively). No isosbestic point is present. (B) Normalized plots of absorbance ratios (A_{max}/A_{450}) of BDT as a function of BS concentration. The absorbance ratio is a measure of the ratio of BDT molecules bound to BS molecules, normalized for unbound BDT. A_{max} values of 50 mM BS solutions with BDT were 416 nm for NaTC (●), 420 nm for NaTDHC (△), NaTDC (□), and NaTCDC (○), and 422 nm for NaTUDC (▲) (other conditions as described for panel A). (C) UV–visible absorption spectra of aqueous 100 μM BDT with 6 M urea (no added NaCl) in the presence of various concentrations of NaTDC (23 ± 1 °C, pH 7.6–8.0, path length of 2 mm). The numbered spectra correspond to NaTDC concentrations of 0, 1.7, 3.3, 8, 25, and 50 mM (1–6, respectively). A tight isosbestic point is present at 427 nm.

NaTC (Figure 5A, left panel) now becomes λ_{max}, and its A value increases progressively with increases in micellar BS concentration. Similar sets of spectra were obtained with other micellar BS; no isosbestic point was evident in this (Figure 5A, right panel) or other micellar BS–BDT spectra (data not shown). Moreover, the blue-shifted λ_{max} differed between micellar BS species, occurring at 416 nm (NaTC), 420 nm (NaTDC, NaTCDC, and NaTDHC) and 422 nm (NaTUDC). In the spectra of NaTDHC, a bile salt that probably remains monomeric in the concentration range studied,[32] an isosbestic point occurs.

Figure 5B displays absorbance ratios (A_{max}/A_{450}) for BDT solutions as a function of BS concentration, where A_{450} is derived from the λ_{max} of BDT monomers (H_2O, 23 ± 1 °C). The curves are similar, with steep increases at low BS concentrations and a leveling off at micellar BS concentrations. The slopes show a gradual change in the concentration range (3–10 mM) where micellization occurs.[33−35,46] Although the A_{max}/A_{450} ratios describe a continuum, the UV–vis spectral evidence suggests a more abrupt phenomenon, hallmarked by the loss of the isosbestic point when micellar BS solutions form (Figure 5A, right panel).

Figure 5C demonstrates the effect of urea on BDT–BS interactions. Shown are UV–vis spectra of 100 μM BDT in 1.7–50 mM NaTDC solutions to which 6 M urea had been added (23 ± 1 °C). With increasing NaTDC concentrations, A_{max} decreases and a new λ_{max} develops at 420 nm. This λ_{max} was identical to that of BDT with monomeric BS without urea [Figure 5A(a), left panel], and all of the spectra, including that of 50 mM NaTDC, intersect at an isosbestic point (427 nm) identical to that of BDT with BS monomers (Figure 5A, left panel). It is apparent, therefore, that 6 M urea prevents BDT self-aggregation, inhibiting 50 mM NaTDC from forming micelles in water,[32] but does not dissociate BS–BDT heterodimers. This is evidenced by the new λ_{max} and tight isosbestic point, consistent with the absorbance equilibria of BDT–NaTDC heterodimers only (compare the left panel of Figure 5A with Figure 5C).

To clarify BDT–BS interactions further, the top panels of Figure 6A display difference spectra for 100 μM BDT with monomeric NaTDC (left panel) (0.5–3.5 mM) and NaTC (right panel) (0.5–5 mM) in H_2O at 23 ± 1 °C (see Methods). In a similar format, the bottom panels display difference spectra for micellar NaTDC (left panel) and NaTC (right panel) (7.5–15 mM). Because difference spectra represent the UV–vis contributions from pure BDT subtracted from those of BS–BDT mixtures, blue-shifted positive peaks represent the relative gain in amplitude when BDT binds BS molecules, whereas red-shifted negative troughs correspond to amplitude loss when free BDT monomers are removed from solution by binding BS. The top panels of Figure 6A show that the amplitude of the blue-shifted peaks increases progressively with increases in the monomeric BS concentration and is accompanied by a deepening of the troughs and the occurrence of an isosbestic point at 427 nm. When micelles form (Figure 6A, bottom panels), λ_{max} shifts slightly to the red [NaTDC (shown) and NaTUDC and NaTDHC (similar data not shown)] or blue (NaTC), but amplitudes display little change.

Figure 6B plots these data, showing that λ_{max} shifts sharply at 6 mM NaTC, 3.5 mM TDC, 10.0 mM TUDC, and 17 mM TDHC, all values that correlate with the conventional spectra, as well as the consensus CMC values of the BS in pure H_2O.[34] The curves also show that 100 μM BDT does not appreciably

DOI: 10.1021/bi501251v
Biochemistry 2015, 54, 1542–1557

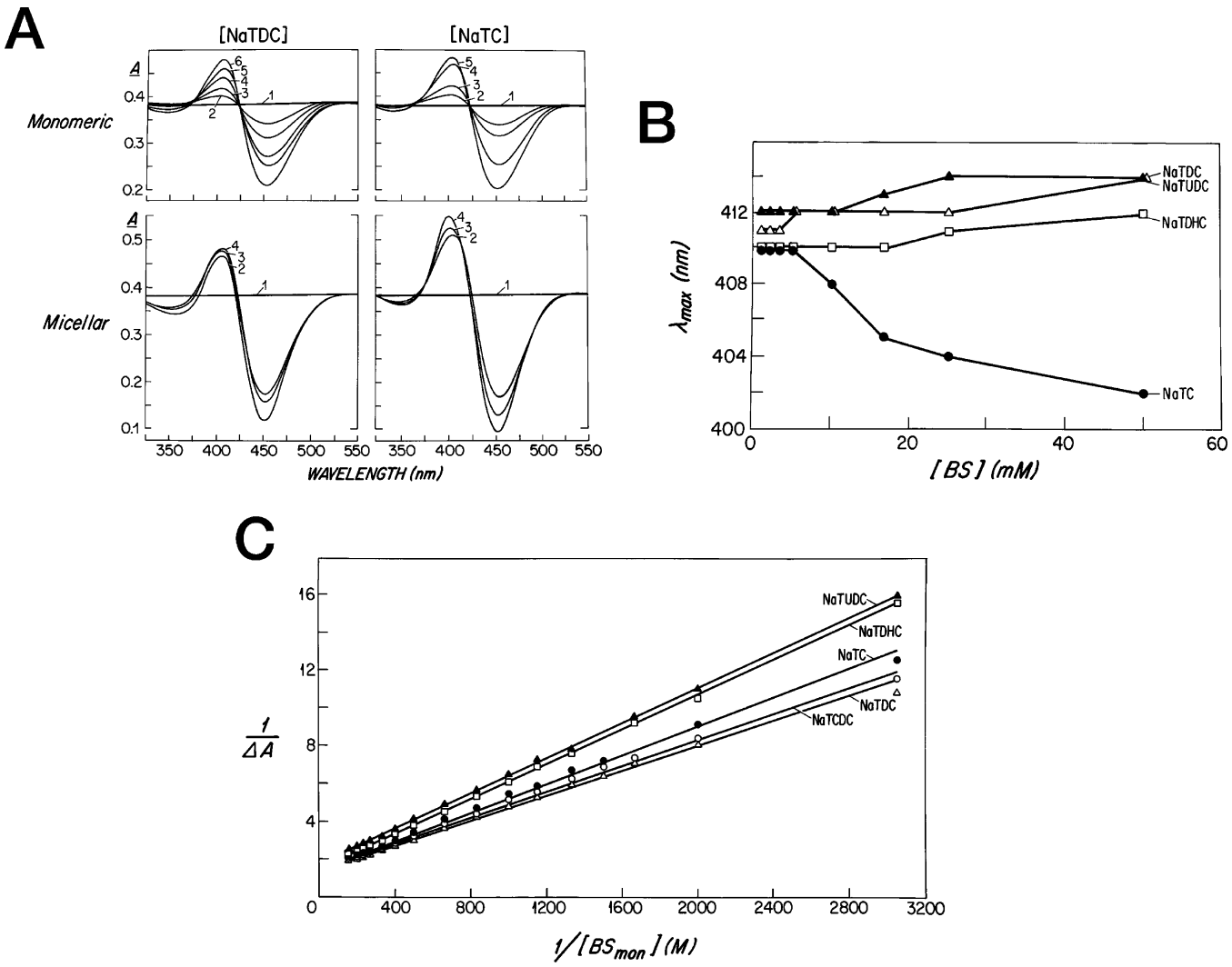

Figure 6. Elucidating BDT−BS interactions by means of difference spectra. (A) UV−visible spectra of 100 μM BDT in monomeric (top) and micellar (bottom) forms at concentrations of NaTDC and NaTC (other conditions as in the legend of Figure 5A). Both reference and sample cuvettes contained 100 μM BDT (path length of 2 mm). The sample cuvette also contained either monomeric NaTDC, with numbered spectra corresponding to concentrations of 0, 0.5, 1, 2, 2.5, and 3.5 mM (1−6, respectively), or monomeric NaTC with numbered spectra corresponding to BS concentrations of 0, 0.5, 1, 3, and 5 mM (1−5, respectively); bottom panels display spectra of micellar NaTDC, with numbered spectra corresponding to concentrations of 0, 7.5, 10, and 15 mM (1−4, respectively), and micellar NaTC, with numbered spectra corresponding to concentrations of 0, 7.5, 10, and 15 mM (1−4, respectively). The positive peaks shift progressively to the blue as functions of micellar BS concentration but not monomeric BS concentration. The vertical scale was offset in the positive direction, so that negative absorption could be registered on the chart paper. The true zero line (#1) is placed at A = 0.38. (B) Values of BDT's λ_{max} from difference spectra (A) plotted as a function of BS concentration. From top to bottom at the left, the curves correspond to NaTUDC (▲), NaTDC (△), NaTDHC (□), and NaTC (●), respectively. Break points occur at BS concentrations of 10 mM TUDC, 3.5 mM TDC, 17 mM TDHC, and 6 mM TC, corresponding to the consensus critical micellar concentrations (CMCs), which are unaltered in the presence of the bile pigment. Conditions were identical to those described for Figure 5A. (C) Double-reciprocal plots of $1/\Delta A$ vs $1/$[BS monomer] from difference spectra with 100 μM BDT (A). ΔA is the absorbance difference at λ_{max} for a 10 mm path length. Binding constant K_D was calculated from the intercept on the x-axis. All values correspond to BS concentrations that lie between 2 and 3 mM. The curves represent NaTUDC (▲), NaTDHC (□), NaTC (●), NaTCDC (○), and NaTDC (△).

alter the CMCs of any BS compared with those measured noninvasively.[34] Because an isosbestic point exists in the spectra of BDT with BS monomers, the most parsimonious interpretation of these results indicates the presence of only two absorbing species in submicellar BS systems, most likely BDT monomers and BDT−BS heterodimers. Because the CMC of BS remains uninfluenced by 100 μM BDT, it is likely that the binding site for BDT molecules resides on the hydrophilic OH-subtending surfaces of BS monomers.

To provide quantitative information about the BS−BDT heterobinding interactions, Figure 6C displays double-reciprocal plots of $1/\Delta A_{max}$ versus $1/$[BS monomer]. For all monomeric BS species, the data points fall on straight lines. However, double-reciprocal plots for micellar BS−BDT heterodimers were not linear and are not displayed. The binding constants (K_D), which are given by $-1/$[BS monomer] at the x-intercept, decrease modestly in the following order: NaTC (2.9 mM) > NaTUDC (2.7 mM) > NaTDHC (2.6 mM) > NaTCDC (2.4 mM) > NaTDC (2.2 mM).

Influence of Temperature and Time on BDT−BS Interactions. At temperatures above 45 °C, UV−vis spectra of BDT in BS solutions were difficult to obtain because BDT

DOI: 10.1021/bi501251v
Biochemistry 2015, 54, 1542−1557

oxidized rapidly, i.e., from orange-yellow to green (biliverdin ditaurate), as verified spectrophotometrically. Oxidation was especially prominent with NaTC and least so, if it occurred at all, with NaTUDC and NaTUC. Oxidation was much slower at temperatures below 37 °C, especially when light and atmospheric O_2 were excluded rigorously, and was prevented entirely for at least 2−3 h at room temperature (23 ± 1 °C). We prepared five oxygenated 200 μM BDT solutions, with and without 50 mM BS, which were incubated in the dark at 37 °C for 48 h. At that time, BDT in NaTC exhibited a dark green color, BDT with NaTDC and NaTCDC showed only a green tint, whereas BDT in NaTUDC remained golden-yellow. Spectrophotometrically, the green color correlated with formation of a λ_{max} of 666 nm after 2 h, reaching a maximum at 48 h, suggesting that BDT had oxidized in part to biliverdin ditaurate (data not shown). In contrast, the spectra of BDT with 50 mM NaTUDC did not manifest these changes, although a slow time-dependent decrease in A_{max} without a λ_{max} shift occurred. After 6 weeks, NaTUC, the trihydroxy 7β isomer of NaTC, which is monomeric in a 50 mM solution,[35] displayed similar protective behavior in preventing BDT oxidation. In striking contrast, BDT in H_2O or in a NaTC solution oxidizes rapidly and spontaneously to biliverdin ditaurate. The antioxidant properties of TUDC, its glycine analogue, or unconjugated UDCA have now been well documented *in vitro*[47] and *in vivo*.[48]

Fluorescence Emission Spectra of Aqueous BDT and BDT−BS Solutions. Figure 7A consecutively displays fluorescence emission spectra of 40 μM BDT with increasing NaCl concentrations (0−300 mM). In contrast to the absorption λ_{max} (Figure 4B), no spectral shift in λ_{max} emission occurs, but the relative fluorescence intensities (RFI) decrease appreciably. Figure 7B displays emission spectra of 40 μM BDT in H_2O with increasing NaTDC concentrations (0−50 mM) consecutively, which result in a progressive increase in RFI. Not displayed are analogous data for BDT with NaTC in H_2O, where RFI increases in proportion to BS concentration but to a lesser degree than with NaTDC. These emission spectra (Figure 7A,B) help discriminate between ionic strength effects of BS, NaCl effects, and specific BS anion effects on BDT fluorescence. Panels C and D of Figure 7, in consecutive numbers, depict the emission spectra of 40 μM BDT with increasing concentrations (0−50 mM) of NaTC and NaTDC, respectively, in 150 mM NaCl. With 50 mM NaTDC, RFI values increased by a factor of 4, whereas in equimolar NaTC solutions, they increased by a factor of 2; however, both are greatly augmented by added NaCl compared to H_2O (compare panel B with panel D of Figure 7). To assess BDT's mobility in micellar BS solutions, steady state fluorescence anisotropy measurements were performed on the same BDT−BS systems (see Methods). With 50 mM NaTDC, added NaCl decreases the anisotropy (from 0.274 to 0.230), suggesting an increase in BDT mobility. In contrast, with 50 mM NaTC, a much smaller decrease in BDT's anisotropy (from 0.300 to 0.291) occurs. Overall, these results suggest that the BDT molecules are much less constrained in or on BS micelles than in predominantly monomeric and dimeric BDT solutions.

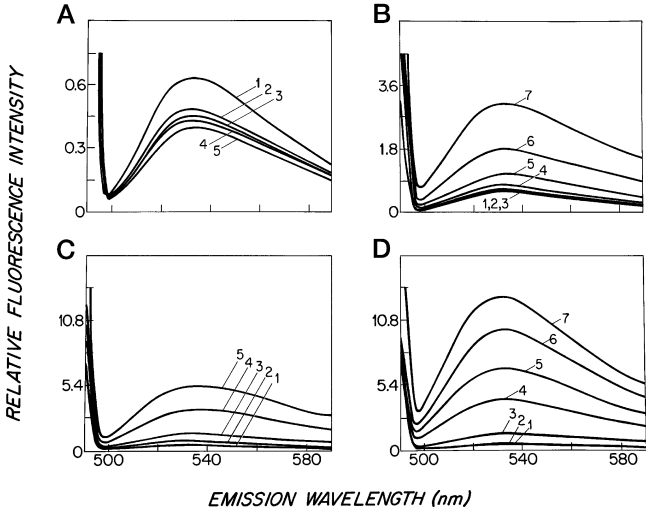

Figure 7. Fluorescence emission spectra of 40 μM BDT, with an excitation wavelength of 490 nm, as a function of added NaCl and/or BS. Numbered spectra correspond to (A) NaCl concentrations of 0, 50, 100, 200, and 300 mM (1−5, respectively), (B) NaTDC concentrations of 0, 1, 2.5, 5, 10, 25, and 50 mM (1−7, respectively) in H_2O, (C) NaTC concentrations of 0, 5, 10, 25, and 50 mM (1−5, respectively) with 150 mM NaCl, and (D) NaTDC concentrations of 0, 1, 2.5, 5, 10, 25, and 50 mM (1−7, respectively) with 150 mM NaCl. Excitation and emission slit widths were 10 and 5 nm, respectively (23 ± 1 °C, pH 7.6−8.0). Florescence is quenched progressively when NaCl is added to BDT alone but enhanced sequentially when BS are present in high micellar concentrations, indicative of BDT disaggregation and monomeric BDT binding to BS micelles.

Circular Dichroism Spectra of BDT−BS Mixtures. Figure 8A displays the CD spectra of 50 μM BDT with 50 mM BS as a function of BS species. The CD spectra of BDT alone or with NaCl fall on the mean residual ellipticity line of zero (θ = 0 deg cm^2 dmol^{-1}). With NaTC and NaTDC, a biphasic curve is obtained in the BDT spectrum; positive ellipticity occurs at longer wavelengths [θ_{477} = 4.3 × 10^5 (NaTDC), and θ_{466} = 2.8 × 10^5 (NaTC)], with negative Cotton effects at shorter wavelengths [θ_{412} = −3.8 × 10^5 (NaTDC), and θ_{415} = −2.6 × 10^5 (NaTC)]. NaTCDC produces a weak negative Cotton effect in BDT (θ_{455} = −1.4 × 10^5), with an even weaker positive Cotton effect at approximately θ_{500}, whereas NaTUDC exhibits a triphasic CD spectrum, with BDT showing two negative θ values and one positive θ value.

Panels B−E of Figure 8 display CD spectra of 50 μM BDT in 50 mM BS solutions as a function of the increasing NaCl concentration. With BDT and 50 mM NaTDC added (Figure 8B), NaCl did not appreciably influence the CD spectra, whereas BDT's Cotton effects with NaTC micelles decreased with an increasing NaCl concentration (Figure 8C). Figure 8D indicates that, for NaTUDC micelles, the negative Cotton effects of BDT at the higher wavelengths (see Figure 8A) became more pronounced. Figure 8E shows that NaCl induces a slight positive Cotton effect in BDT between 460 and 510 nm. Unlike BDT, which is insensitive to pH,[15] UCB changes its ionization state as a function of pH.[10,49] Therefore, we varied pH values (Figure 8F) from 10.5 to 6.9 to obtain CD spectra of 50 μM UCB in 50 mM NaTDC. With a decreasing pH, UCB changes from dianion to monoanion and then to diacid; in accordance with this, positive Cotton effects at the longer wavelengths become negative (pH ≤8.5), and concomitantly, the negative Cotton effects at the shorter wavelengths develop a positive sign.

DOI: 10.1021/bi501251v
Biochemistry 2015, 54, 1542−1557

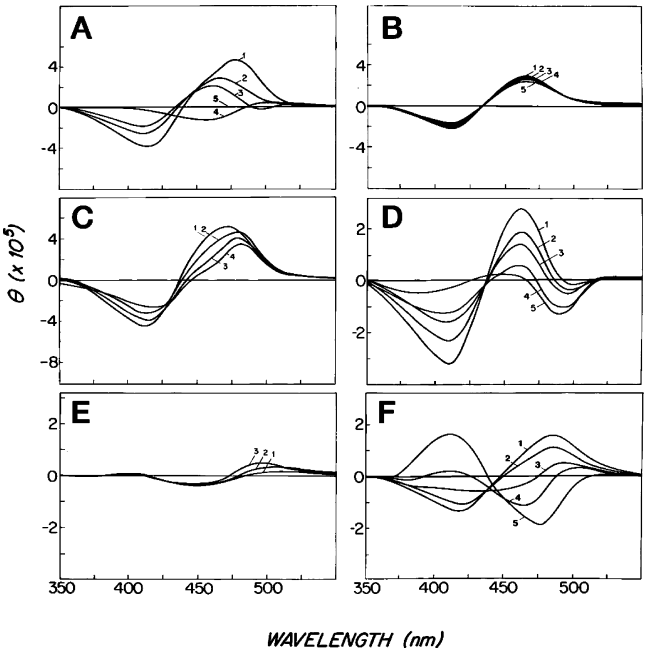

Figure 8. Circular dichroism (CD) spectra of 50 μM BDT (A–E) and 50 μM UCB (F) under various solution conditions. The CD spectrum of 50 μM BDT alone or dianionic 50 μM UCB, with and without NaCl, falls on the θ = 0 deg cm^2 dmol^{-1} line (A-4, B-6, D-6, F-3). (A) CD spectra of BDT with 50 mM NaTC (1), NaTDC (2), NaTUDC (3), and NaTCDC (5). (B) CD spectra of BDT with 50 mM NaTDC and increasing NaCl concentrations of (1) 0 mM, (2) 150 mM, (3) 300 mM, (4) 600 mM. and (5) 1 M. (C) CD spectra of BDT with 50 mM NaTC and increasing NaCl concentrations of (1) 0 mM, (2) 150 mM, (3) 600 mM, and (4) 1 M. (D) CD spectra of BDT with 50 mM NaTUDC and increasing NaCl concentrations of (1) 0 mM, (2) 150 mM, (3) 300 mM, (4) 600 mM, and (5) 1 M. (E) CD spectra of BDT in NaTCDC with increasing NaCl concentrations of (1) 0 mM, (2) 300 mM and (3) 1 M. (F) CD spectra of 50 μM UCB (unconjugated bilirubin IXα) with 50 mM NaTDC as a function of solution pH, (1) 6.9, (2) 7.7, (4) 8.5, (5) 9.5, and (6) 10.5, showing inversions as the pH is increased. The sensitivity in experiments A–C and E was 0.05 and in experiments D and F was 0.02 (23 ± 1 °C, pH 7.6–8.0 for BDT and pH 6.9–10.5 for UCB).

DISCUSSION

For defining the physical chemistry of any conjugated bile pigment, it became clear that BDT, a natural compound found in biles of certain fish, is manifestly an excellent analogue of fully ionized bilirubin diglucuronide, the principal cBR in human bile.[1,17] BDT has two taurine side chains amide-linked to the C8 and C12 propionic acids of UCB, approximately the same length as glucuronic acids. In contrast to the latter, they are not chemically labile as ester linkages are and subtend acid-resistant sulfonate groups.[17] The two carboxylic acid groups of bilirubin diglucuronide at C8 and C12, by virtue of their vicinal ester linkages, should have comparable properties, because the acidic functions are much stronger than the propionate side chains of UCB. The major chemical divergences are the six hydroxyl groups of glucuronides, which are bulky but, as is typical of other sugars and uronic acids, are not well hydrated in aqueous systems. BDT exhibits many biochemical and physiological properties of bilirubin diglucuronide, such as similar UV–absorption spectra,[17,31] forms azo pigments with diazotized sulfanilic acid,[50] migrates chromatographically with R_f values similar to those of native cBR,[30,51] and is efficiently secreted into bile of Sprague-Dawley and Gunn rats when injected intravenously.[52,53] The singular and indeed curious physiological property of BDT is that it is well secreted in mutant Wistar rats with dysfunction of the canalicular multiple organic anion transporter (cMOAT), now named formally MRP2/ABCC2, that transports cBR across the canalicular membrane of the liver.[54] Notwithstanding these comparisons, the solution properties of any cBR have not been studied heretofore. Furthermore, BDT is a native bilirubin conjugate[20,21] worthy of detailed physicochemical study for its own sake.

Spectral Characteristics of BDT Constitutional Isomers. Our BDT (Figure 1) consisted of two additional constitutional isomers (≈25%; putatively BDT IIIα and BDT XIIIα, cf. McDonagh and Assisi[27]) in addition to the natural BDT IXα isomer. These constitutional isomers were most likely formed by disproportionation[55] during laboratory conjugation with taurine. In this regard, it is noteworthy that UCB (Figure 1) from the same source contained 94, 4, and 2% of the IXα, IIIα, and XIIIα isomers, respectively (see Materials). As was found with commercial UCB,[27] these BDT constitutional isomers also cocrystallize with the IXα isomer of BDT[4] and cannot be separated preparatively by conventional methods.

The UV–vis spectra of the dioctylamine salts of BDT in excess dioctylamine/MeOH mixture were different, as evidenced by the three isomers displayed in Figure 2A. The blue 420 nm shoulder was most pronounced in the spectrum of presumptive BDT XIIIα compared with IIIα and IXα. Even in 6 M urea (Figure 4C) and in very low monomeric concentrations (Figure 2B, left panel), this blue shoulder persists and is not indicative of self-aggregation of the molecules[22,56] but represents an intrinsic property of BDT isomers. It occurs because the two pyrromethenone chromophores in each half-molecule require different energies for their π–π^* orbital transitions.[25] These energy levels depend upon the substituents and the medium, and the so-called "exciton splitting" gives rise to a broad λ_{max} band with a variable blue shoulder in the UV–vis spectra.[4,56,57] The "exciton splitting" effect falls off with the inverse cube of the distance between the chromophores and is smallest when they are coplanar.[22] In the crystal structure, the interplanar angle in the "ridge-tile" conformation of UCB IXα can range from 98° to 104° (summarized in ref 17) and is expected to be much greater in solution.[58] Therefore, the spectra in Figure 2A suggest that the "ridge-tile" dihedral angle is smallest in solutions of BDT XIIIα, the putative endovinyl isomer, and largest in solutions of BDT IIIα, the putative exovinyl isomer.[22] Because of the internal consistency of these data, the isomer mixture apparently behaved as a "single" component. Therefore, the results obtained with the constitutional isomer mixture would be unlikely to differ appreciably from the self-aggregation properties of BDT IXα alone.

Physical Chemistry of BDT Self-Association. In contrast to the monomeric BDT spectra, the blue-shifted shoulder at 415 nm, the magnitude of which progressively increased with increases in BDT concentration (Figure 2B), is caused by self-aggregation of BDT molecules. Charge shielding with added NaCl facilitated self-association and was accompanied by a decrease in RFI (Figure 7). Nonetheless, self-aggregation was proven unequivocally in the analytic ultracentrifugation experiments (Figure 3A,B) when dimers formed at low concentrations and tetramers at higher (low millimolar) concen-

DOI: 10.1021/bi501251v
Biochemistry 2015, 54, 1542–1557

trations. As inferred from the UV−vis spectra and verified in the sedimentation equilibrium experiments, the tight isosbestic point at 423 nm that occurred with increasing BDT concentrations in H_2O (Figure 2B) and with added NaCl (Figure 4B) is strongly indicative of a monomer−dimer equilibrium. Many dyes,[59] porphyrins, metalloporphyrins, and open-chain tetrapyrroles (reviewed by Carey and Spivak[17]), including UCB,[60] dimerize at very low aqueous concentrations and fluoresce only weakly because of quenching of emitted light from fast molecular collisions in solution. It is of interest that sedimentation equilibrium studies of aqueous UCB at pH 8.5, when ionization may be incomplete,[61,62] showed oligomerization to pentamers[60,63] and at pH 10, when UCB is fully ionized,[36] oligomerization to primarily dimers and tetramers,[63] paralleling the results presented here for a cBR at pH 7.6−8.0. In the case of porphyrins, however, self-aggregation of hydrophobic species can be extensive and may be open-ended (reviewed by Carey and Spivak).[17]

With fully ionized porphyrins, the dimerization constants at 25 °C (reviewed in ref 17) appear to correlate with the hydrophilic−hydrophobic balance of the molecules.[64] Protoporphyrin shows the largest K_D (3.1×10^6 M^{-1}) and coproporphyrin the smallest (9.8×10^3 M^{-1}), the latter being rather similar to the K_D for BDT at 23 °C (2×10^3 M^{-1}). In this study, the ΔH_D values for BDT (Table 1) also approximate the dimerization value (−6.1 kcal/mol) of dianionic hematoporphyrin.[64]

BDT dimerization was a highly facilitated process, as evidenced by large negative ΔG_D values (Table 1). The relatively large negative values for ΔH_D and constant $T\Delta S_D$ values at temperatures ranging from 5 to 50 °C (Table 1) and the profound effect of added NaCl and 6 M urea were consistent with an isodesmic reaction, driven mainly by hydrophobic interactions and minimally counteracted by negative charge−charge (sulfonate) repulsive forces. It is possible that BDT self-association may be stabilized by $\pi-\pi$ forces or mediated partly via H-bonding with water molecules because aromatic π-H-bonds are unusually strong (further discussed below with reference to BDT−BS dimers).[65] This is consistent with observations of dimers of other ionic dyes,[66] UCB−dimethyl sulfoxide interactions, and molecular packing of solvated molecules in crystalline bilirubin IXα salts (see the summary in ref 17). At higher BDT concentrations (Figure 3A), the second equilibrium appears to be between dimers and tetramers because trimers are unlikely on the basis of the ultracentrifugation experiments (Figure 3B). Because the "ridge-tile" conformation of bile pigments is maintained in solution[67] as it is in dianionic UCB, any model of BDT self-aggregation must allow maximal separation of the negative charges and preservation of the lowest-free energy state of the binary tetrapyrroles. This would be maintained by a dihedral angle in the vicinity of 100° between the dipyrromethenone chromophores. Therefore, to explain the size limit of BDT tetramers at high concentrations and at high NaCl concentrations and to satisfy the absence of a CD spectrum (Figure 8), a double "bookend−bookend" conformation involving four BDT molecules alternating as pairs of P(+) and M(−) enantiomers would fulfill all requirements and would minimize sulfonate charge repulsion (Figure 9). This structure also shows why trimeric self-association is unlikely (see Figure 3A,B). A model in which stacks of BDT "ridge-tiles" are interleaved with similar but inverted stacks in the same conformation, such as what occurs in the unit cell of crystalline UCB IXα[68] or its diisopropylammonium salt (see ref 17), was also considered. This model was discounted, nonetheless, because, if BDT tetramers were so arranged, the charged groups would be vicinal and there would be no *a priori* reason why self-association should be limited to tetramers.

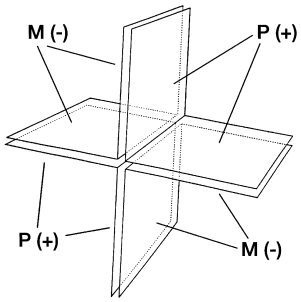

Figure 9. Proposed tetrameric structure of BDT as ridge-tiles in double-bookend formation. It is presumed that 2P(+) and 2M(−) enantiomers alternate in the formation of the limiting tetramer, which is facilitated by a decrease in temperature, added NaCl, and an increase in BDT concentration. However, millimolar solutions of BS even well below the CMC disaggregate the entire ensemble fully in that the equilibrium is shifted to BDT monomers bound tightly to BS monomers, and to BS micelles above their respective CMCs.

Physical Chemistry of Interactions of BDT with Bile Salt Monomers. Spectroscopic[36] and enzymatic peroxidation studies[69] have suggested that, when fully ionized (pH ∼10) or partially undissociated (pH 8.2), UCB IXα binds to BS monomers and micelles. We suggested previously[36] that the binding site for fully ionized UCB appears to be the polar face of BS monomers and small BS (NaTC) micelles, whereas at higher BS concentrations, fully ionized UCB monomers may migrate into a hydrophobic region of BS micelles. Monoanionic UCB appears to interact hydrophobically and may even "co-micellize" with BS micelles.[70] To date, no analogous information about a cBR has been published. In the work presented here, extensive spectroscopic data suggest that heterodimer formation between BDT and BS monomers is of very high affinity. Because pathophysiological concentrations were simulated, millimolar BS dissociated self-aggregates of micromolar BDT essentially completely. Therefore, by shifting the binding equilibria, monomers, and especially micellar BS, appear to "break" BDT dimers and higher-order aggregates in solution. We can summarize the reasons for these concepts as follows. First, the isosbestic point at 427 nm (Figure 5A, left panel) in the presence of BS monomers differed by 4 nm from the isosbestic point observed during BDT dimerization (423 nm) (Figure 2B, right panel). Second, the addition of 6 M urea inhibited BDT self-association (Figure 4C) but did not inhibit the formation of the blue-shifted shoulder or alter the new λ_{max} in the presence of BS monomers (Figure 5C), both indicative of BS−BDT heterodimers. Third, the addition of increasing monomeric concentrations of BS to a monomer−dimer equilibrium of BDT did not lead to further quenching of fluorescence as in BDT dimerization but rather enhanced fluorescence (Figure 7B−D). Fourth, the tight isosbestic points in the spectra of BDT-BS monomers as well as in 50 mM BS solutions with 6 M urea (Figure 5A,C) indicate the presence of only two BDT-absorbing species, most likely BDT monomers and BDT−BS heterodimers.

These arguments notwithstanding, it is worth considering in detail why these binary aggregates cannot be "broken" by 6 M urea and why the binding forces of BDT−BS heterodimers

DOI: 10.1021/bi501251v
Biochemistry 2015, 54, 1542−1557

must be considerably stronger than those of BDT homodimers or even BS micelles. It is likely that powerful π-electron H-bond forces are responsible for stabilization of BDT−BS heteroaggregates. Aromatic π-electrons of pyrrole rings, such as in BDT molecules, are capable of bonding with water molecules or to the hydroxyl groups of BS with energies of −3.4 to −3.8 kcal/mol.[65] The binding energy involved in a single bond of this type is equivalent to the total binding energy (−3.4 to −3.8 kcal/mol) involved in small primary micelle formation by NaTC and NaTDC at 20 °C[71,72] and only ∼1 kcal/mol less than the energy of BDT dimerization itself (Table 1). Hence, because of multiple hydroxyl substituents, the extraordinarily strong forces that stabilize BDT−BS heterodimers are likely to be two or three π-orbital H-bonds (generating 6.8−1.4 kcal/mol at 20 °C) between the BDT's pyrrole rings and the di- and trihydroxyl groups of BS monomers. Because the blue shoulder in the UV−vis spectrum with monomeric BDT−BS binding is indicative of hydrophilic bonding, either directly or via H_2O molecules or via the H-bonds of BDT, the extent of the shift should provide information about the molecular packing of the two molecules. The blue shift in BDT was most pronounced with NaTC (416 nm), a BS of intermediate hydrophilicity with three α-oriented OH groups and showing no "sharp" CMC.[73] In contrast, the blue shift is smaller with NaTDC and NaTCDC (420 nm) and is smallest with NaTUDC (422 nm). This suggests that a 7β-OH group[74,75] with its equatorial orientation might be inappropriate for maximizing π-orbital H-bonds with BDT concomitantly with a 3α-OH group, possessed by all natural BS.[16,46,72] It seems that two α-oriented OH groups, and preferably three α-OH groups on one side of the BS molecule, are ideal for achieving this end. Apparently, aromatic π-orbital H-bonds require orientation of the H atom toward the center of the aromatic ring, and this has been shown to be typically 3.2−3.8 Å in centrosymmetric or vertical distance.[65]

The K_D values of BDT−BS monomer heteroassociations (Figure 6C) were similar, falling between 2 and 3 mM for all BS, which approximate the estimated CMCs of dihydroxy BS.[34,76] However, this is not the case with NaTC. Because of its relatively high "CMC" value (7.5 mM in H_2O[34,76]), which is thrice the K_D value, the capacity of NaTC monomers for BDT binding should be far superior to that of all other common BS.

Physical Chemistry of Interactions of BDT with BS Micelles. With micellar BS solutions, an equilibrium occurred among three molecular species of BDT (probably BDT monomers, BDT−BS heterodimers, and BDT−BS micelles) as evidenced by the absence of an isosbestic point in the spectra of BS−BDT micelles (Figure 5A, right panel). BDT's interactions with BS micelles stand in contrast to those of the common porphyrins, UCB, or BMG, which typically lodge in hydrophobic domains of micellar BS, as evidenced by the red-shifted UV−vis spectra.[34] In the work presented here, blue shift in λ_{max} of BDT occur at the CMC of most BS species, irrespective of BDT concentration (as shown for NaTC in the right panel of Figure 5A). This is likely to be a result of strong hydrophilic interactions between micellar BS and BDT monomers, together with a BDT−BS heterodimer with micellar interaction in a microenvironment that remains identical to BDT and BS monomers when micellization occurs. This notion is further supported by the marked blue shift in λ_{max} of BDT with NaTC (Figure 5B), suggesting that the micellar environment of BDT is more hydrophilic when it is bound to NaTC micelles than to NaTDC or NaTCDC micelles. What is distinct, nonetheless, are the red-shifted λ_{max} values for BDT with micellar NaTUDC, suggesting partitioning of BDT into a more hydrophobic micellar environment reminiscent of what occurs with BMG and NaTCDC.[77] As noted for the antioxidant effect and the fluorescent and CD spectra, NaTUDC, the most hydrophilic of the common BS,[78,79] with one OH group in position 3α and a second in equatorial position 7β,[75] appears to interact with BDT in a tighter conformation and a more hydrophobic microenvironment compared to those of the other common BS.[75,78] Evidence to bolster this line of reasoning is that among all BS micellar species, the capacity of NaTUDC to bind BDT is the smallest (Figure 5B), and in the BDT difference spectra, the largest λ_{max} shift when BS micellization occurs (Figure 6B) is between NaTC (402 nm) and NaTUDC (414 nm).

The closing argument for hydrophilic binding of BDT to BS micelles is provided by CD spectra (Figure 8). All BS-induced optical activity in BDT is analogous to phenomena well-known in the cases of UCB−albumin,[80,81] UCB−cyclodextrin,[82] and UCB−deoxycholate complexes.[83−85] With UCB binding (and presumably also with BDT), the origin of optical activity[25] is most likely due to the preferred selection of one P(+) or M(−) enantiomer over the other[86,87] and, thus, induction of Cotton effects with positive or negative chirality.[57] To reveal how modulation of the hydrophobic−hydrophilic balance of a bile pigment can illuminate bile pigment−BS interactions, the pH variation study with UCB and micellar NaTDC was highly instructive. Although UCB is a soluble amphiphile at high pH, it becomes insoluble at low pH because of the sequestration of all its polar functions in six intramolecular H-bonds (Figure 1). At high pH [>8.3 (see Figure 8)], when UCB becomes dianionic, the Cotton effects[85] were identical to those of BDT at pH 7.6−8.0, whereas at low pH (<8.3), where more than 90% of the UCB was monoanionic and formation of the diacid UCB begins, Cotton effects were inverted (see also ref 84). The dominant micellar binding site for UCB depends on BS concentration, BS species, and pH, as inferred from UV−vis spectra.[36,69,70] At lower pH (<8.3) and high BS concentrations, the hydrophobic BS micelle interior probably becomes the predominant binding site, whereas at high pH (>8.3), the hydrophilic surface is apparently preferred, as it is with BDT at neutral pH (this work). The preferred conformational state of diacid UCB in the hydrophobic BS micelle interior is not known but should be distinctly different from that which is bound to the exterior of a BS micelle.

Variable Cotton effects in the CD spectra of BDT (Figure 8) with a congener series of taurine-conjugated BS may be explained by variations in the "exciton coupling" of BDT's pyrromethanone chromophores. Maximal "exciton coupling" interactions are believed to occur when the chromophores are set at a 90° angle and are weakest at wide or narrow angles.[25] The CD experiments suggest that the geometric conformation of the BDT chromophores is closest to a 90° angle in the presence of NaTC, followed by a wider angle with NaTDC and NaTCDC. Intramolecular H-bonding in BDT may be quite complex, in that H-bonding may involve the amide function of the conjugating group, and even the sulfonic acids, with the pyrrolic NH groups.[67] These variations in intramolecular H-bonding would tend to flatten BDT molecules and reduce or invert the CD spectrum of BDT, like that with NaTCDC micelles (Figure 8E). Although in unbound form a folded "ridge-tile" conformation is the minimal energy state for BDT,[22,88] interactions with BS molecules may easily change

DOI: 10.1021/bi501251v
Biochemistry 2015, 54, 1542−1557

this. Clearly, on the basis of several lines of physicochemical evidence presented here, this is uniquely different for BS with a 7β-OH function and, on the basis of several lines of physicochemical evidence presented in this work, is manifested particularly by BDT's resistance to oxidation induced by the equatorial 7β function (see also refs 47 and 48).

The lack of sensitivity of BDT to oxidation at the central CH_2 bridge in NaTUDC and NaTUC systems was surprising and unanticipated. It is believed that relief from conformational strain and not necessarily an adnexal O_2 attack facilitates biliverdin formation.[4] Fluorescence anisotropy indicates that BDT is held loosely in a "ridge-tile" conformation by NaTC and therefore more easily oxidized but is flattened and conformationally strained by NaTUDC, with oxidation being prevented. An additional factor is that O_2 is less soluble in lipid than in water, so the central CH_2 bridge of the pyrromethenone unit might be exposed to a more hydrophilic domain in NaTC micelles than in a more hydrophobic but exterior micellar domain in NaTUDC micelles. We can discount the possibility that BDT is bound tightly inside a structured NaTUDC micelle[89] because we have produced several lines of evidence in this work to indicate that the BDT binding site is with the OH-studded surface of the micelle. Furthermore, 50 mM NaTUC is monomeric in H_2O[35] yet displayed the same antioxidant effect as micellar NaTUDC.

Pathophysiological and Biological Implications. Natural mixtures of cBR occur in human and animal biles,[6] and mixed BS micelles are more complex than single-BS micelles;[33,34,46] however, some cautious deductions can be made on the basis of our *in vitro* physicochemical results with BDT and pure BS. Hepatocellular secretion of cBR into bile occurs via the ABC transporter MRP2/ABCC2.[54,90] Transport against a concentration gradient into the canaliculus may be facilitated, and back-diffusion from the biliary tree prevented, by tight monomeric binding of cBR to BS monomers and micelles. Extensive BDT−BS binding would explain the almost total lack of osmotic activity of secreted cBR in bile *in vivo* over wide concentration ranges.[11,12] In view of the large concentration differential (at least 1:10) between biliary cBR and BS,[16] it is unlikely that self-aggregates of cBR will exist in the bulk aqueous water of native bile.[16,17]

It is believed that enterohepatic circulation of UCB, not evident in health, can be induced by any condition that causes increased spillage of BS into the large intestine.[91,92] Therefore, the properties of binding of cBR to BS monomers and micelles in the cecum and proximal colon may play as yet unidentified roles in bacterial β-glucuronidase hydrolysis, modulating biliverdin and urobilinogen formation, aqueous solubility, and calcium binding, all of which influence passive absorption of UCB from the intestine.[92] Recycling of UCB from the gut increases biliary levels of cBR and blood levels of UCB, resulting in a propensity to pigment gallstone formation and jaundice from elevated bile pigment levels in these fluids. The nature and extent of binding of cBR and UCB to BS monomers and micelles in bile may play crucial roles in influencing endogenous or bacterial β-glucuronidase hydrolysis, calcium complex formation, and calcium bilirubinate precipitation culminating in pigment gallstones.[9] Clearly, further work is required to define the influence, if any, of physiological concentrations of the biliary phospholipids, calcium, and cholesterol on these BDT−BS interactions.

Bilirubin IXα is a potent antioxidant.[93,94] Presumably, the binding of cBR to BS micelles in bile would bring the bile pigments into the proximity of polyunsaturated phospholipids and cholesterol cosolubilized within mixed BS micelles and vesicles. Thereby, cBR will be in an appropriate location and physical state to protect unsaturated biliary lipids from oxidation.[16,95] Indeed, no oxidized lipids are detected in sterile, fresh gallbladder biles of humans or animals.[95,96] As we have shown here, BS with equatorial 7β-OH functions apparently protect cBR itself from oxidation. This may be important in animals such as bears and hystricomorpha that enter prolonged hibernations.[97,98] In this connection, it has been known for nearly two millennia that bear bile possesses hepatoprotective properties.[98,99] The concept behind this Chinese folk remedy has present-day currency in that NaTUDC or its glycine-conjugated analogue (now prescribed as the unconjugated free acid) is the active principle.[100] The time-honored way of determining whether a bear's bile was of good medicinal value was to allow bile in the extirpated and opened gallbladder to dry in air; if the bile remained amber-colored, it was potent, but biles containing predominantly more common BS changed from yellow to green or black and were discarded as being of no medicinal use.[98,99] This study suggests that NaTUDC-rich native bile remains amber-colored because 7β-OH BS inhibit oxidation of cBR. Interestingly, dried pig bile, often sold fraudulently as "bear" bile in the Orient,[98] has large quantities of the hydrophilic conjugates of hyodeoxycholate and hyocholate,[100] whose steroid nuclei subtend equatorial 6α-OH groups.[101] It might be of interest, therefore, to determine whether BS subtending 6α-hydroxy groups also prevent spontaneous cBR oxidation.

In summary, the intriguing hybrid interactions between fully ionized cBR and bile salt conjugates are highly complex physicochemically, attaching to bile no additional osmotic activity, strong hydrophilic bonding in an aqueous environment, and, depending upon the bile salt species, such as those with an equatorial 7-OH function, exhibiting powerful antioxidant activity just like bilirubin IXα itself and possibly being proactive throughout the gastrointestinal tract; although BDT is found in high concentrations only in certain fishes, the same phenomena are to be anticipated with all cBR, including bilirubin mono- and diglucuronides in human bile.

AUTHOR INFORMATION

Corresponding Author

*Brigham and Women's Hospital, 75 Francis St., Boston, MA 02115. E-mail: mcarey@partners.org. Fax: (617) 730-5807. Phone: (617) 732-5822.

Present Address

[†]M.W.N.: Krankenhaus Maria Stern, Am Anger 1, Remagen 53424, Germany. E-mail: neubrand@krankenhaus-remagen.de.

Funding

Supported in part by National Institutes of Health Grants DK036588 and DK034854 (M.C.C.), National Science Foundation Grants BBS 86-15815 and DIR9002027 (T.M.L.), and Deutsche Forschungsgemeinschaft Fellowship Ne345/1-1 (M.W.N.).

Notes

The authors declare no competing financial interest.

ACKNOWLEDGMENTS

We graciously thank Dr. Barton Holmquist and the late Dr. Bert Vallee for hospitality in their laboratories, Drs. Martin Reers and Judith Storch for generous advice about fluorescence

DOI: 10.1021/bi501251v
Biochemistry 2015, 54, 1542−1557

spectroscopy, Ms. Theresa M. Ridgeway for expert technical assistance with analytical ultracentrifugation, Monika R. Leonard for superb editing, and Laura Wohn for word processing.

■ ABBREVIATIONS

cBR, conjugated bilirubin(s); UCB, unconjugated bilirubin; BDT, bilirubin ditaurate; BS, bile salt(s); TC, taurocholate; TUC, taurourso(7-epi)cholate; TUDC, tauroursodeoxycholate; TDC, taurodeoxycholate; TCDC, taurochenodeoxycholate; TDHC, taurodehydro(triketo)cholate; RFI, relative fluorescence intensity; CD, circular dichroism; λ_{max}, wavelength of maximal absorption; *A*, absorbance.

■ REFERENCES

(1) Bissell, D. M. (1986) Heme catabolism and bilirubin formation. In *Bile Pigments and Jaundice: Molecular, Metabolic and Medical Aspects* (Ostrow, J. D., Ed.) pp 133−156, Marcel Dekker, New York.

(2) Ostrow, J. D., and Murphy, N. H. (1970) Isolation and properties of conjugated bilirubin from bile. *Biochem. J. 120*, 311−327.

(3) Ostrow, J. D. (1990) Unconjugated bilirubin and cholesterol gallstone formation. *Hepatology 12*, 219S−226S.

(4) McDonagh, A. F. (1979) Bile pigments: Bilatrienes and 5,15-biladienes. In *The Porphyrins* (Dolphin, D., Ed.) Vol. *6*, pp 293−491, Academic Press, New York.

(5) Gordon, E. R., Chan, T. H., Samodai, K., and Goresky, C. A. (1977) The isolation and further characterization of the bilirubin tetrapyrroles in bile-containing human duodenal juice and dog gallbladder bile. *Biochem. J. 167*, 1−8.

(6) Spivak, W., and Carey, M. C. (1985) Reverse-phase h.p.l.c. separation, quantification and preparation of bilirubin and its conjugates from native bile. Quantitative analysis of the intact tetrapyrroles based on h.p.l.c. of their ethyl anthranilate azo derivatives. *Biochem. J. 225*, 787−805.

(7) Spivak, W., and Yuey, W. (1986) Application of a rapid and efficient h.p.l.c. method to measure bilirubin and its conjugates from native bile and in model bile systems. Potential use as a tool for kinetic reactions and as an aid in diagnosis of hepatobiliary disease. *Biochem. J. 234*, 101−109.

(8) Gordon, E. R., and Goresky, C. A. (1982) A rapid and quantitative high performance liquid chromatographic method for assaying bilirubin and its conjugates in bile. *Can. J. Biochem. 60*, 1050−1057.

(9) Cahalane, M. J., Neubrand, M. W., and Carey, M. C. (1988) Physical-chemical pathogenesis of pigment gallstones. *Semin. Liver Dis. 8*, 317−328.

(10) Spivak, W., DiVenuto, D., and Yuey, W. (1987) Non-enzymic hydrolysis of bilirubin mono- and diglucuronide to unconjugated bilirubin in model and native bile systems. Potential role in the formation of gallstones. *Biochem. J. 242*, 323−329.

(11) Apstein, M. D., and Robins, S. J. (1982) Effect of organic anions on biliary lipids in the rat. *Gastroenterology 83*, 1120−1126.

(12) Gartner, L. M., Lane, D. L., and Cornelius, C. E. (1971) Bilirubin transport by liver in adult *Macaca mulatta*. *Am. J. Physiol. 220*, 1528−1535.

(13) Scharschmidt, B. F., and Schmid, R. (1978) The micellar sink: A quantitative assessment of the association of organic anions with mixed micelles and other macromolecular aggregates in rat bile. *J. Clin. Invest. 62*, 1122−1131.

(14) Tazuma, S., and Holzbach, R. T. (1987) Transport of conjugated bilirubin and other organic anions in bile: Relation to biliary lipid structures. *Proc. Natl. Acad. Sci. U.S.A. 84*, 2052−2056.

(15) Tazuma, S., Barnhart, R. L., Reeve, L. E., Tokumo, H., and Holzbach, R. T. (1988) Biliary secretion of organic anions in the dogs: Association with defined lipid particles. *Am. J. Physiol. 255*, G745−G751.

(16) Carey, M. C., and Duane, W. C. (1994) Enterohepatic Circulation. In *The Liver: Biology and Pathobiology* (Arias, I. M., Boyer, J. L., Fausto, N., Jacoby, W. B., Schachter, D., and Shafritz, D. A., Eds.) 3rd ed., pp 719−767, Raven Press, New York.

(17) Carey, M. C., and Spivak, W. (1986) Physical chemistry of bile pigments and porphyrins with particular references to bile. In *Bile Pigments and Jaundice: Molecular, Metabolic and Medical Aspects* (Ostrow, J. D., Ed.) pp 81−132, Marcel Dekker, New York.

(18) Compernolle, F. (1982) Bilirubin conjugates; isolation, structure analysis and synthesis. In *Bilirubin, Volume 1, Chemistry* (Heirwegh, K. P. R., and Brown, S. B., Eds.) pp 59−73, CRC Press, Boca Raton, FL.

(19) Jirsa, M., Večerek, B., and Ledvina, M. (1956) Di- and monotaurobilirubin similar to a directly reacting form of bilirubin in serum. *Nature 177*, 895.

(20) Sakai, T., Watanabe, K., and Kawatsu, H. (1987) Occurrence of ditaurobilirubin, bilirubin conjugated with two moles of taurine, in the gallbladder bile of yellowtail, *Seriola quinqueradiata*. *J. Biochem. 102*, 793−796.

(21) Tenhunen, R. (1965) Studies on bilirubin and its metabolism. *Ann. Med. Exp. Biol. Fenn. 43* (Suppl.6), 1−45.

(22) Falk, H. (1989) *The chemistry of linear oligopyrroles and bile pigments*, pp 1−621, Springer, New York.

(23) Lightner, D. A., Gawronski, J. K., and Wijekoon, W. M. D. (1987) Complementarity and chiral recognition: Enantioselective complexation of bilirubin. *J. Am. Chem. Soc. 109*, 6354−6362.

(24) Puzicha, G., Pu, Y. M., and Lightner, D. A. (1991) Allosteric regulation of conformational enantiomerism. Bilirubin. *J. Am. Chem. Soc. 113*, 3583−3592.

(25) Person, R. V., Peterson, B. R., and Lightner, D. A. (1994) Bilirubin conformational analysis and circular dichroism. *J. Am. Chem. Soc. 116*, 42−59.

(26) McDonagh, A. F., Palma, L. A., Lauff, J. J., and Wu, T. W. (1984) Origin of mammalian biliprotein and rearrangement of bilirubin glucuronides in vivo in the rat. *J. Clin. Invest. 74*, 763−770.

(27) McDonagh, A. F., and Assisi, F. (1971) Commercial bilirubin: A trinity of isomers. *FEBS Lett. 18*, 315−317.

(28) Pope, J. L. (1967) Crystallization of sodium taurocholate. *J. Lipid Res. 8*, 146−147.

(29) Hsu, W. P. (1986) Micellar growth in solutions of synthetic and biological surfactants. Ph.D. Dissertation, Clarkson University, Potsdam, NY.

(30) Kratohvil, J. P., and DelliColli, H. T. (1968) Micellar properties of bile salts. Sodium taurodeoxycholate and sodium glycodeoxycholate. *Can. J. Biochem. 46*, 945−952.

(31) Doumas, B. T., Wu, T. W., Poon, K. C., and Jendrzejczak, B. (1985) Chemical nature of a synthetic bilirubin conjugate and its reactivities in the total and direct reactions by the Jendrassik-Gróf method. *Clin. Chem. 31*, 1677−1682.

(32) Small, D. M. (1968) Size and structure of bile salt micelles: Influence of structure, concentration, counterion concentration, pH and temperature. *Adv. Chem. Ser. 84*, 31−52.

(33) Carey, M. C. (1985) Physical-chemistry properties of bile acids and their salts. In *New Comprehensive Biochemistry: Volume 12 Sterols and Bile Acids* (Danielsson, H., and Sjövall, J., Eds.) pp 345−403, Elsevier, Amsterdam.

(34) Cabral, D. J., and Small, D. M. (1989) Physical chemistry of bile. In *Handbook of Physiology: The Gastrointestinal System III* (Schultz, S. G., Forte, J. G., and Rauner, B. B., Eds.) pp 621−662, American Physiology Society-Waverly Press, Philadelphia.

(35) Roda, A., Hofmann, A. F., and Mysels, K. J. (1983) The influence of bile salt structure on self-association in aqueous solutions. *J. Biol. Chem. 258*, 6362−6370.

(36) Carey, M. C., and Koretsky, A. P. (1979) Self-association of unconjugated bilirubin-IXα in aqueous solution at pH 10.0 and physical-chemical interactions with bile salt monomers and micelles. *Biochem. J. 179*, 675−689.

(37) Knudsen, A., Pedersen, A. O., and Brodersen, R. (1986) Spectroscopic properties of bilirubin-human serum albumin com-

DOI: 10.1021/bi501251v
Biochemistry 2015, 54, 1542−1557

plexes: A stoichiometric analysis. *Arch. Biochem. Biophys. 244*, 273−284.
(38) Birdsall, B., King, R. W., Wheeler, M. R., Lewis, C. A., Jr., Goode, S. R., Dunlap, R. B., and Roberts, G. C. (1983) Correction for light absorption in fluorescence studies of protein-ligand interactions. *Anal. Biochem. 132*, 353−361.
(39) Lakowicz, J. R. (1983) *Principles of Fluorescence*, pp 111−153, Plenum, New York.
(40) Williams, R. C., Jr. (1978) Continuous laser optics in the ultracentrifuge. In *Methods in Enzymology*, Vol. *48*, pp 185−191, Academic Press, New York.
(41) Yphantis, D. A. (1964) Equilibrium ultracentrifugation of dilute solutions. *Biochemistry 3*, 297−317.
(42) Laue, T. M. (1981) Rapid precision interferometry for the analytical ultracentrifuge. Ph.D. Dissertation, University of Connecticut, Storrs, CT.
(43) Chervenka, C. H. (1970) *A Manual of Methods for the Analytical Ultracentrifuge*, pp 69−72, Spinco Division of Beckman Instruments, Palo Alto, CA.
(44) Johnson, M. L., Correia, J. J., Yphantis, D. A., and Halvorson, H. R. (1981) Analysis of data from the analytical ultracentrifuge by nonlinear least-squares techniques. *Biophys. J. 36*, 575−588.
(45) Yphantis, D. A., and Waugh, D. F. (1956) Ultracentrifugal characterization by direct measurement activity. I. Theoretical. *J. Phys. Chem. 60*, 623−629.
(46) Small, D. M. (1971) The physical chemistry of cholanic acids. In *The Bile Acids: Chemistry, Physiology and Metabolism, Volume 1, Chemistry* (Nair, P. P., and Kritchevsky, D., Eds.) pp 249−356, Plenum Press, New York.
(47) Lapenna, D., Ciofani, G., Festi, D., Neri, M., Pierdomenico, S. D., Giamberardino, M. A., and Cuccurullo, F. (2002) Antioxidant properties of ursodeoxycholic acid. *Biochem. Pharmacol. 64*, 1661−1667.
(48) Gaspar, J. M., Martins, A., Cruz, R., Rodrigues, C. M., Ambrósio, A. F., and Antiago, A. R. (2013) Tauroursodeoxycholic acid protects retinal neural cells from cell death induced by prolonged exposure to elevated glucose. *Neuroscience 253*, 380−388.
(49) Vítek, L., and Ostrow, J. D. (2009) Bilirubin chemistry and metabolism; harmful and protective aspects. *Curr. Pharm. Des. 15*, 2869−2883.
(50) Jirsa, M., Ledvina, M., and Večerek, B. (1958) Neue Bilirubinderivate, II Chromatographie der Azofarbstoffe des direkten Bilirubins und des Taurobilirubins mit inversen Phasen. *Hoppe-Seyler's Z. Physiol. Chem. 311*, 93−95.
(51) Jirsa, M., and Večerek, B. (1958) Neue Bilirubinderivate. I. Ihr Vergleich mit Gallen-und Serum-Bilirubin. *Hoppe-Seyler's Z. Physiol. Chem. 311*, 87−92.
(52) Jirsa, M., and Hykes, P. (1978) Taurobilirubin metabolism and excretion in rats. *Sb. Lek. (1887-2003) 80*, 49−51.
(53) Apstein, M. D. (1984) Inhibition of biliary phospholipid and cholesterol secretion by bilirubin in the Sprague-Dawley and Gunn rat. *Gastroenterology 87*, 634−638.
(54) Verkade, H. J., Havinga, R., Gerding, A., Vonk, R. J., and Kuipers, F. (1993) Mechanism of bile acid-induced biliary lipid secretion in the rat: Effect of conjugated bilirubin. *Am. J. Physiol. 264*, G462−G469.
(55) Heirwegh, K. P. M., and Blanckaert, N. (1982) Analytical chemistry of rubins. In *Bilirubin Volume 1. Chemistry* (Heirwegh, K. P. M., and Brown, S. B., Eds.) pp 125−151, CRC Press, Boca Raton, FL.
(56) Lightner, D. A. (1982) Structure, photochemistry and organic chemistry of bilirubin. In *Bilirubin Volume 1. Chemistry* (Heirweigh, K. P. M., and Brown, S. B., Eds.) pp 1−58, CRC Press, Boca Raton, FL.
(57) Harada, N., and Nakanishi, K. (1983) Circular dichroic spectroscopy: Exciton coupling. In *Organic Stereochemistry*, pp 1−28, University Science Books, Mill Valley, CA.
(58) Yang, B. J., Morris, M. D., Xie, M. Q., and Lightner, D. A. (1991) Resonance Raman spectroscopy of bilirubins: Band assignments and application to bilirubin/lipid complexation. *Biochemistry 30*, 688−694.
(59) Rabinowitch, E., and Epstein, L. F. (1941) Polymerization of dyestuffs in solution. Thionine and methylene blue. *J. Am. Chem. Soc. 63*, 69−78.
(60) Wolf, S. (1980) Structure of bilirubin in solution. M.S. Thesis, University of Nevada, Reno, NV.
(61) Ostrow, J. D., Celic, L., and Mukerjee, P. (1988) Molecular and micellar associations in the pH-dependent stable and metastable dissolution of unconjugated bilirubin by bile salts. *J. Lipid Res. 29*, 335−348.
(62) Hahm, J. S., Ostrow, J. D., Mukerjee, P., and Celic, L. (1992) Ionization and self-association of unconjugated bilirubin determined by rapid solvent partition from chloroform, with further studies of bilirubin solubility. *J. Lipid Res. 33*, 1123−1137.
(63) Lai, B. (1984) I. Photooxidation studies of pyrroles, pyrromethanones and bilirubin monitored by a micro-oxygen electrode. II. Aggregation of bilirubin in solution from ultracentrifugation studies. M.S. Thesis, University of Nevada, Reno, NV.
(64) Karns, G. A., Gallagher, W. A., and Elliot, W. B. (1979) Dimerization constants of water-soluble porphyrins in aqueous alkali. *Bioorg. Chem. 8*, 69−81.
(65) Atwood, J. L., Hamada, F., Robinson, K. D., Orr, G. W., and Vincent, R. L. (1991) X-ray diffraction evidence for aromatic π hydrogen bonding to water. *Nature 349*, 683−684.
(66) Valdes-Aguilera, O., and Neckers, D. C. (1989) Aggregation phenomena in xanthene dyes. *Acc. Chem. Res. 22*, 171−177.
(67) Lightner, D. A., Adams, T. C., and Ma, J. S. (1984) Bilirubin mono- and bis-dimethylamides. Synthesis, spectroscopy and solution structures. *Tetrahedron 40*, 4253−4260.
(68) Bonnett, R., Davies, J. E., Hursthouse, M. B., and Sheldrick, G. M. (1978) The structure of bilirubin. *Proc. R. Soc. B 202*, 249−268.
(69) Rege, R. V., Webster, C. C., and Ostrow, J. D. (1988) Interactions of unconjugated bilirubin with bile salts. *J. Lipid Res. 29*, 1289−1296.
(70) Ostrow, J. D., Celic, L., and Mukerjee, P. (1991) Unconjugated bilirubin (B) dianions "co-micellize" with taurocholate (TC). Evidence from partition of B from $CHCl_3$ into aqueous TC solutions at pH = 9.0. *Hepatology 14*, 150A.
(71) Carey, M. C., and Small, D. M. (1969) Micellar properties of dihydroxy and trihydroxy bile salts: Effects of counterion and temperature. *J. Colloid Interface Sci. 31*, 382−396.
(72) Mazer, N. A., Carey, M. C., Kwasnick, R. F., and Benedek, G. B. (1979) Quasielastic light scattering studies of aqueous biliary lipid systems. Size, shape, and thermodynamics of bile salt micelles. *Biochemistry 18*, 3064−3075.
(73) Kratohvil, J. P., Hsu, W. P., Jacobs, M. A., Aminabhavi, T. M., and Mukunoki, Y. (1983) Concentration-dependent aggregation patterns of conjugated bile salts in aqueous sodium chloride solutions. A comparison between sodium taurodeoxycholate and sodium taurocholate. *Colloid Polym. Sci. 261*, 781−785.
(74) Carey, M. C., Montet, J. C., Phillips, M. C., Armstrong, M. J., and Mazer, N. A. (1981) Thermodynamic and molecular basis for dissimilar cholesterol-solubilizing capacities by micellar solutions of bile salts: Cases of sodium chenodeoxycholate and sodium ursodeoxycholate and their glycine and taurine conjugates. *Biochemistry 20*, 3637−3648.
(75) Lindley, P. F., and Carey, M. C. (1987) Molecular packing of bile acids. Structure of ursodeoxycholic acid. *J. Cryst. Spectrosc. Res. 17*, 231−249.
(76) Cohen, D. E., and Carey, M. C. (1990) Rapid (1 h) high performance gel filtration chromatography resolves coexisting single micelles, mixed micelles, and vesicles in bile. *J. Lipid Res. 31*, 2103−2112.
(77) Spivak, W., Morrison, C., Devinuto, D., and Yuey, W. (1988) Spectrophotometric determination of the critical micellar concentration of bile salts using bilirubin monoglucuronide as a micellar probe. Utility of derivative spectroscopy. *Biochem. J. 252*, 275−281.
(78) Carey, M. C. (1983) Measurement of the physical-chemical properties of bile salt solutions. In *Bile Acids in Gastroenterology*

DOI: 10.1021/bi501251v
Biochemistry 2015, 54, 1542−1557

(Barbara, L., Dowling, R. H., Hofmann, A. F., and Roda, E., Eds.) pp 19−56, MTP Press, Lancaster, PA.
(79) Armstrong, M. J., and Carey, M. C. (1982) The hydrophobic-hydrophilic balance of bile salts. Inverse correlation between reverse-phase high performance liquid chromatographic mobilities and micellar cholesterol-solubilizing capacities. *J. Lipid Res. 23*, 70−80.
(80) Lightner, D. A., Reisinger, M., and Landen, G. L. (1986) On the structure of albumin-bound bilirubin. Selective binding of intramolecularly hydrogen-bonded conformational enantiomers. *J. Biol. Chem. 261*, 6034−6038.
(81) Lightner, D. A., Wijekoon, W. M. D., and Zhang, M. H. (1988) Understanding bilirubin conformation and binding. Circular dichroism of human serum albumin complexes with bilirubin and its esters. *J. Biol. Chem. 263*, 16669−16676.
(82) Lightner, D. A., Gawronski, J. K., and Gawronska, K. (1985) Conformational enantiomerism in bilirubin. Selection by cyclodextrins. *J. Am. Chem. Soc. 107*, 2456−2461.
(83) Perrin, J. H., and Wilsey, M. (1971) The induced optical activity of bilirubin in the presence of sodium deoxycholate. *J. Chem. Soc. D*, 769−770.
(84) Reisinger, M., and Lightner, D. A. (1985) Bilirubin conformational enantiomer selection in sodium deoxycholate chiral micelles. *J. Inclusion Phenom. 3*, 479−485.
(85) Puranam, K. L., and Balaram, P. (1987) Solubilization of bilirubin by cholate micelles. Spectroscopic and gel permeation studies. *Proc.—Indian Acad. Sci., Chem. Sci. 98*, 453−468.
(86) Le Bas, G., Allegret, A., Mauguen, Y., de Rango, C., and Bailly, M. (1980) The structure of triclinic bilirubin chloroform-methanol solvate. *Acta Crystallogr. B36*, 3007−3011.
(87) Blauer, G., and Wagnière, G. (1975) Conformation of bilirubin and biliverdin in their complexes with serum albumin. *J. Am. Chem. Soc. 97*, 1949−1954.
(88) Geddes, A. J., Potterton, E., and Willis, G. (1980) Steric hindrance in proposed photoisomers of bilirubin. *Photochem. Photobiol. 31*, 337−340.
(89) Kawamura, H., Murata, Y., Yamaguchi, T., Igimi, H., Tanaka, M., Sugihara, G., and Kratohvil, J. P. (1989) Spin-label studies of bile salt micelles. *J. Phys. Chem. 93*, 3321−3326.
(90) Jansen, P. L. M., Peters, W. H., and Lamers, W. H. (1985) Hereditary chronic conjugated hyperbilirubinemia in mutant rats caused by defective hepatic anion transport. *Hepatology 5*, 573−579.
(91) Brink, M. A., Méndéz-Sánchez, N., and Carey, M. C. (1996) Bilirubin cycles enterohepatically after ileal resection in the rat. *Gastroenterology 110*, 1945−1957.
(92) Vítek, L., and Carey, M. C. (2003) Enterohepatic cycling of bilirubin as a cause of 'black' pigment gallstones in adult life. *Eur. J. Clin. Invest. 33*, 799−810.
(93) Stocker, R., and Ames, B. N. (1987) Potential role of conjugated bilirubin and copper in the metabolism of lipid peroxides in bile. *Proc. Natl. Acad. Sci. U.S.A. 84*, 8130−8134.
(94) Stocker, R., Yamamoto, Y., McDonagh, A. F., Glazer, A. N., and Ames, B. N. (1987) Bilirubin is an antioxidant of possible physiological importance. *Science 235*, 1043−1046.
(95) Hay, D. W., and Carey, M. C. (1990) Chemical species of lipids in bile. *Hepatology 12*, 6S−14S.
(96) Hay, D. W., Cahalane, M. J., Timofeyeva, N., and Carey, M. C. (1993) Molecular species of lecithins in human gallbladder bile. *J. Lipid Res. 34*, 759−768.
(97) Hagey, L. R., Crombie, D. L., Espinosa, E., Carey, M. C., Igimi, H., and Hofmann, A. F. (1993) Ursodeoxycholic acid in the Ursidae: Biliary bile acids of bears, pandas, and related carnivores. *J. Lipid Res. 34*, 1911−1917.
(98) Wang, D. Q., and Carey, M. C. (2014) Therapeutic uses of animal biles in traditional Chinese medicine: An ethnopharmacological, biophysical chemical and medicinal review. *World J. Gastroenterol. 20*, 9952−9975.
(99) Makino, I., and Takebe, K. (1982) Bear bile and ursodeoxycholic acid. *Sogo Rinsho 31*, 2385−2387.
(100) Hofmann, A. F. (1994) Bile Acids. In *The Liver: Biology and Pathobiology* (Arias, I. M., Boyer, J. L., Fausto, N., Jakoby, W. B., Schachter, D., and Shafritz, D. A., Eds.) 3rd ed., pp 677−718, Raven Press, New York.
(101) Hall, S. R., Maslen, E. N., and Cooper, A. (1974) The crystal and molecular structure of 3α,6α-dihydroxy-5β-cholan-24-oic acid, $C_{24}O_4H_{40}$. *Acta Crystallogr. B30*, 1441−1447.

DOI: 10.1021/bi501251v
Biochemistry 2015, 54, 1542−1557